

GENERATIVE DIFFUSION MODELING

A Practical Handbook

Authors:

Zihan Ding
Chi Jin

zihand@princeton.edu
chij@princeton.edu

Abstract

This handbook offers a unified perspective on diffusion models, encompassing diffusion probabilistic models, score-based generative models, consistency models, rectified flow, and related methods. By standardizing notations and aligning them with code implementations, it aims to bridge the “paper-to-code” gap and facilitate robust implementations and fair comparisons. The content encompasses the fundamentals of diffusion models, the pre-training process, and various post-training methods. Post-training techniques include model distillation and reward-based fine-tuning. Designed as a practical guide, it emphasizes clarity and usability over theoretical depth, focusing on widely adopted approaches in generative modeling with diffusion models.

Contents

1	Introduction	2
2	Diffusion Model Basics	4
2.1	Problem Formulation	4
2.2	Diffusion Model	5
2.2.1	Fundamentals	5
2.2.2	Training	9
2.2.3	Inference	13
2.3	Consistency Model	14
2.3.1	Training	15
2.3.2	Inference	17
2.4	Rectified Flow	18
2.4.1	Training	18
2.4.2	Inference	19
2.4.3	InstaFlow-prediction	19
2.4.4	Distillation	22
2.4.5	Velocity Mapping	23
2.5	TrigFlow	24
2.5.1	Training	24
2.5.2	Inference	25
2.6	Prediction Parameterization	25
2.6.1	ϵ -prediction and x -prediction in Diffusion Model	26
2.6.2	v -prediction in Diffusion Model	27
2.6.3	v -prediction in Rectified Flow	27
2.6.4	ϵ -prediction and x -prediction in Rectified Flow	29
2.6.5	f -prediction in Consistency Model	29
2.7	Unified Formulation	29
3	Diffusion Generation	31
3.1	Pre-training	31
3.1.1	Diffusion Model	31
3.1.2	Consistency Model	32

3.1.3	Rectified Flow	32
3.1.4	TrigFlow	32
3.2	Distillation	33
3.2.1	Progressive Distillation	33
3.2.2	Score Distillation Sampling	34
3.2.3	Variational Score Distillation	34
3.2.4	Distribution Matching Distillation	35
3.2.5	Adversarial Diffusion Distillation	38
3.2.6	Consistency-based Distillation	39
3.3	Reward-based Fine-tuning	41
3.3.1	Direct Reward Gradient	41
3.3.2	Gradient-free Reward Optimization	42

1 Introduction

Diffusion models [Sohl-Dickstein et al., 2015, Song and Ermon, 2019, Ho et al., 2020, Song et al., 2021] have recently revolutionized generative modeling, achieving remarkable advancements in generating images [Rombach et al., 2022, Ramesh et al., 2022], audio [Liu et al., 2023a, Polyak et al., 2024], video [Brooks et al., 2024, Polyak et al., 2024], 3D content [Poole et al., 2022, Wang et al., 2024c], and even 4D representations [Wang et al., 2024b]. Despite this rapid progress, existing research often presents the concepts and notations of diffusion models in inconsistent ways, even when the underlying methodologies are similar. Compounding this issue, the formulations in many papers often differ from their corresponding code implementations or lack sufficient implementation details, creating what is referred to as the “paper-to-code” gap. These inconsistencies make it challenging for practitioners to directly implement methods from the literature, hindering robust implementations and fair cross-method comparisons.

This handbook seeks to provide a unified perspective on various models, collectively referred to here as “diffusion models” as an umbrella term¹. These include diffusion probabilistic models [Sohl-Dickstein et al., 2015, Ho et al., 2020], score-based generative models [Song et al., 2021], consistency models [Song et al., 2023], rectified flow [Liu et al., 2022], flow matching [Lipman et al., 2022], TrigFlow [Lu and Song, 2024], and others. The authors have made every effort to standardize the notations across these methods and align them closely with their code implementations to minimize the paper-to-code gap. Additionally, this handbook aims to clarify the relationships among these different methods, highlighting existing transformations and unifications that connect them.

While diffusion models are theoretically grounded in fields such as non-equilibrium statistical physics, optimal transport, and score matching, this handbook intentionally avoids delving deeply into these theoretical foundations. Instead, its primary purpose is to serve as a practical guide for researchers and practitioners.

It is important to note that this handbook does not aim to provide a comprehensive overview of diffusion models for generative modeling. Rather, it focuses on a subset of the most popular and widely adopted works that are frequently applied in practice.

¹This might be inappropriate, as some may differentiate score-based generative models from diffusion probabilistic models and instead prefer the umbrella term “generative diffusion processes”.

Notations

a, b, c	Vectors or scalars or constants.
\mathbf{A}	A matrix.
$q(x_t x_{t-1})$	Single-step conditional distribution of diffusion process.
$q(x_{t-1} x_t)$	Single-step posterior distribution of denoising process in diffusion.
$p_\theta(x_{t-1} x_t)$	Neural network approximated single-step distribution of denoising process in diffusion.
$q(x)$	Sample distribution of training dataset.
x_0	Clean sample from sample distribution, 0 indicates timestep $t = 0$ in diffusion process.
\hat{x}_0	Predicted clean sample.
x_θ	Predicted clean sample \hat{x}_0 with model parameterized by θ .
$\mathcal{N}(0, \mathbf{I})$	Normal distribution.
ε	Sampled Gaussian noise.
ϵ_θ	Predicted noise with parameterized model by θ .

The above notations are kept consistent across the entire paper.

2 Diffusion Model Basics

2.1 Problem Formulation

We consider samples $x^{(1)}, x^{(2)}, \dots, x^{(n)} \sim q(x)$, and try to fit a parameterized distribution $p_\theta(x)$ from these samples. After that, new samples can be drawn $x \sim p_\theta(x)$.

The classical choice of $p_\theta(x)$ can be Gaussian distributions, Gaussian mixture models, etc.

In general, the maximum likelihood estimation $\max_\theta \sum_i^n \log p_\theta(x = x^{(i)})$ is intractable for the integration in the log-probability estimation:

$$\begin{aligned} \log p_\theta(x) &= \log \int p_\theta(x, z) dz \\ &= \log \int p_\theta(x|z)p(z) dz \end{aligned}$$

Variational inference offers a way:

$$\begin{aligned} \log p_\theta(x) &= \log \int p_\theta(x, z) dz \\ &= \log \int p_\theta(x|z)p(z) dz \\ &= \log \int q_\phi(z|x) \frac{p_\theta(x|z)p(z)}{q_\phi(z|x)} dz \quad (\text{with approximate posterior } q_\phi(z|x)) \\ &\geq \mathbb{E}_{q_\phi(z|x)} [\log p_\theta(x|z) + \log p(z) - \log q_\phi(z|x)] \quad (\text{Jensen's Inequality}) \end{aligned}$$

with the evidence lower bound (ELBO) $\mathcal{L}(\phi, \theta; x) = \mathbb{E}_{q_\phi(z|x)} [\log p_\theta(x|z)] - D_{\text{KL}}(q_\phi(z|x) \| p(z))$ as a tractable objective. With additional loss term $D_{\text{KL}}(q_\phi(z|x) \| p_\theta(z|x))$, it constitutes the variational auto-encoder (VAE) [Kingma, 2013].

Apart from variational autoencoders (VAEs), other generative methods such as energy-based models, normalizing flows, and generative adversarial networks (GANs) offer diverse approaches to estimating the probability distributions of training data. Among these, diffusion models stand out for their exceptional tractability and flexibility.

Definition 2.1 (Diffusion Model) *For the data sampled from distribution $x_0 \sim q(x_0)$, the forward diffusion process corrupts the data distribution to a Gaussian distribution as following:*

$$x_t = \bar{a}_t x_0 + \bar{b}_t \varepsilon, \varepsilon \sim \mathcal{N}(0, \mathbf{I})$$

with $t \in \{1, 2, \dots, T\}$ for discrete-time cases and $t \in [0, T]$ for continuous-time cases. \bar{a}_t and \bar{b}_t are time-dependent coefficients specified by a given noise schedule. The general diffusion models learn the backward process, which is the reverse-time counterpart to the forward diffusion process.

For discrete-time cases, the forward process can be alternatively written as per-step diffusion process as follows. Given $x_0 \sim q(x_0)$, we have the forward diffusion process:

$$x_t = a_t x_{t-1} + b_t \varepsilon_{t-1}, \varepsilon_{t-1} \sim \mathcal{N}(0, \mathbf{I})$$

with $t \in \{1, 2, \dots, T\}$ and existence of the representation of \bar{a}_t and \bar{b}_t by a_t and b_t .

The diffusion process can be characterized as the solution to a stochastic differential equation (SDE), which is commonly expressed in the following general form:

$$dx = f(x, t)dt + g(x, t)dw, \quad (1)$$

where $f(x, t)$ is the drift coefficient, $g(x, t)$ is the diffusion coefficient, w is the standard Wiener process.

An instantiation of diffusion models can select different schedules a_t and b_t . For example, for a discrete-time diffusion process with a variance preserving schedule $a_t = \sqrt{1 - \beta_t}$, $b_t = \sqrt{\beta_t}$, the corresponding SDE is:

$$dx = -\frac{1}{2}\beta_t x dt + \sqrt{\beta_t} dw$$

In diffusion models, there's also often an interest in the backward SDE for sampling, which has the following form for general SDE as Eq. (1) [Anderson, 1982]:

$$dx = [f(x, t) - \nabla_x \cdot [g(x, t)g(x, t)^\top] - g(x, t)g(x, t)^\top \nabla_x \log p_t(x)] dt + g(x, t) d\bar{w}, \quad (2)$$

where $p_t(x)$ is the probability distribution of x_t at diffusion time t , and \bar{w} is a reverse-time Wiener process.

For above SDE, there exists an ordinary differential equation (ODE), with equivalent marginal distribution $p_t(x)$ [Song et al., 2021]:

$$dx = [f(x, t) - \frac{1}{2}\nabla_x \cdot [g(x, t)g(x, t)^\top] - \frac{1}{2}g(x, t)g(x, t)^\top \nabla_x \log p_t(x)] dt$$

In Eq. (2), when $g(x, t)$ does not depend on x , as $g(t)$ in diffusion models, we have a simplified form:

$$dx = [f(x, t) - g(t)g(t)^\top \nabla_x \log p_t(x)] dt + g(t) d\bar{w}, \quad (3)$$

since the divergence $\nabla_x \cdot [g(\cdot, t)g(\cdot, t)^\top] = 0$. The corresponding simplified reverse ODE is:

$$dx = [f(x, t) - \frac{1}{2}g(t)g(t)^\top \nabla_x \log p_t(x)] dt \quad (4)$$

It is observed that estimating the score function, $\nabla \log p_t(x)$, is a crucial requirement in the reverse sampling process, serving as one of the fundamental components of diffusion models.

2.2 Diffusion Model

Diffusion models are a class of generative models that iteratively transform simple noise distributions into complex data distributions through a sequence of forward and reverse processes. This section offers a detailed introduction to the derivation of diffusion model fundamentals, training objectives, and inference mechanisms.

2.2.1 Fundamentals

Suppose the data is sampled from distribution $x_0 \sim q(x_0)$, the diffusion model is trained to generate samples \hat{x}_0 that follow the same distribution, starting from random Gaussian noise. Three important variants are introduced in this section, including denoising diffusion probabilistic model, denoising diffusion implicit model and score-based denoising diffusion.

Denoising Diffusion Probabilistic Model [Ho et al., 2020]. The distribution $q(x_t|x_{t-1}) = \mathcal{N}(x_t; \sqrt{\alpha_t}x_{t-1}, (1 - \alpha_t)\mathbf{I})$ can be written as:

$$\boxed{x_t = \sqrt{\alpha_t}x_{t-1} + \sqrt{1 - \alpha_t}\varepsilon, \varepsilon \sim \mathcal{N}(0, \mathbf{I})} \quad (5)$$

$\beta_t = 1 - \alpha_t$ is the variance of noise added at each step $t \in [T]$.

By chain rule,

$$x_t = \sqrt{\bar{\alpha}_t}x_0 + \sqrt{1 - \bar{\alpha}_t}\varepsilon_0, \varepsilon_0 \sim \mathcal{N}(0, \mathbf{I}) \quad (6)$$

with $\bar{\alpha}_t = \prod_{i=1}^t \alpha_i$. Equivalently, we have $x_t \sim q(x_t|x_0) = \mathcal{N}(x_t; \sqrt{\bar{\alpha}_t}x_0, (1 - \bar{\alpha}_t)\mathbf{I})$. This equation is also used to predict:

$$\boxed{\hat{x}_0 = \frac{1}{\sqrt{\bar{\alpha}_t}}x_t - \frac{\sqrt{1 - \bar{\alpha}_t}}{\sqrt{\bar{\alpha}_t}}\varepsilon_\theta} \quad (7)$$

which is called the Tweedie's formula. ε_θ is the approximated prediction of ε_0 with a parameterized model by θ , conditioning on x_t and t :

$$\varepsilon_\theta(x_t, t) \approx \mathbb{E}_{X_0 \sim q} \left[\frac{1}{\sqrt{1 - \bar{\alpha}_t}}X_t - \frac{\sqrt{\bar{\alpha}_t}}{\sqrt{1 - \bar{\alpha}_t}}X_0 \mid X_t = x_t \right]$$

where X_0, X_1 are generic random variables. The function $\varepsilon_\theta(x_t, t)$ consistently takes x_t and t as conditions; however, for simplicity, these dependencies are omitted in subsequent sections of the paper, like in Eq. (7). We intentionally use distinct notations, ε_θ and ε , throughout the paper. Here, $\varepsilon \sim \mathcal{N}(0, \mathbf{I})$ represents true random variables, while ε_θ denotes their parameterized predictions. Despite both representing noise in the diffusion process, this distinction highlights their respective roles.

The forward diffusion process, as described above, corresponds to the forward stochastic differential equation (SDE) in Eq.(1). Our focus also extends to the reverse diffusion process, commonly referred to as the denoising process, which aligns with the reverse SDE in Eq.(2). In discrete-time scenarios, such as those in DDPM, the posterior probability $q(x_{t-1}|x_t, x_0)$ for a one-step denoising process has an explicit analytical form, which is derived below.

By Bayes' rule, we have the posterior distribution,

$$\begin{aligned} q(x_{t-1}|x_t, x_0) &= \frac{q(x_{t-1}, x_t|x_0)}{q(x_t|x_0)} = \frac{q(x_t|x_{t-1}, x_0)q(x_{t-1}|x_0)}{q(x_t|x_0)} \\ &\propto \mathcal{N}\left(x_{t-1}; \frac{\sqrt{\alpha_t}(1 - \bar{\alpha}_{t-1})x_t + \sqrt{\bar{\alpha}_{t-1}}(1 - \alpha_t)x_0}{1 - \bar{\alpha}_t}, \frac{(1 - \alpha_t)(1 - \bar{\alpha}_{t-1})\mathbf{I}}{1 - \bar{\alpha}_t}\right) \end{aligned} \quad (8)$$

where we assume $q(x_{t-1}|x_t, x_0) = q(x_{t-1}|x_t)$ as a Markov chain with independent random noise ε at each timestep. In above Gaussian distribution, $\mu(x_t, x_0) = \frac{\sqrt{\alpha_t}(1 - \bar{\alpha}_{t-1})x_t + \sqrt{\bar{\alpha}_{t-1}}(1 - \alpha_t)x_0}{1 - \bar{\alpha}_t}$, plug $x_0 = \frac{1}{\sqrt{\bar{\alpha}_t}}x_t - \frac{\sqrt{1 - \bar{\alpha}_t}}{\sqrt{\bar{\alpha}_t}}\varepsilon_0$ (derived from Eq. (6)) into it, we have the posterior mean and variance:

$$\boxed{\mu(x_t, \varepsilon_0) = \frac{1}{\sqrt{\alpha_t}}x_t - \frac{1 - \alpha_t}{\sqrt{1 - \bar{\alpha}_t}\sqrt{\alpha_t}}\varepsilon_0}$$

$$\sigma_t^2 = \frac{(1 - \alpha_t)(1 - \bar{\alpha}_{t-1})}{1 - \bar{\alpha}_t}$$

which is also used for reparameterization between ϵ_θ and μ_θ . ϵ_θ and μ_θ are approximated prediction of ε_0 and $\mu(x_t, \varepsilon_0)$ with parameterized models by θ .

Therefore, by replacing ε_0 with $\epsilon_\theta(x_t, t)$, $q(x_{t-1}|x_t, x_0)$ can also be written as:

$$x_{t-1}(x_t, \epsilon_\theta, \varepsilon) = \frac{1}{\sqrt{\alpha_t}}x_t - \frac{1 - \alpha_t}{\sqrt{1 - \bar{\alpha}_t}\sqrt{\alpha_t}}\epsilon_\theta + \sigma_t\varepsilon \quad (9)$$

which is the Langevin dynamics sampling from x_t to x_{t-1} , with $\sigma_t^2 = \frac{(1-\alpha_t)(1-\bar{\alpha}_{t-1})}{1-\bar{\alpha}_t}$, $\varepsilon \sim \mathcal{N}(0, \mathbf{I})$. σ_t^2 is sometimes also set to just $1 - \alpha_t$ [Ho et al., 2020] due to similar experimental performances.

Plug Eq. (7) into Eq. (9),

$$\begin{aligned} x_{t-1}(x_t, \hat{x}_0, \varepsilon) &= \frac{1}{\sqrt{\alpha_t}}x_t - \frac{1 - \alpha_t}{\sqrt{1 - \bar{\alpha}_t}\sqrt{\alpha_t}}\left[\frac{x_t - \sqrt{\bar{\alpha}_t}\hat{x}_0}{\sqrt{1 - \bar{\alpha}_t}}\right] + \sigma_t\varepsilon \\ \Leftrightarrow x_{t-1}(x_t, \hat{x}_0, \varepsilon) &= \frac{\sqrt{\bar{\alpha}_{t-1}}(1 - \alpha_t)}{1 - \bar{\alpha}_t}\hat{x}_0 + \frac{\sqrt{\alpha_t}(1 - \bar{\alpha}_{t-1})}{1 - \bar{\alpha}_t}x_t + \sigma_t\varepsilon \end{aligned} \quad (10)$$

Note that Eq. (9) is also equivalently written as the following in DDIM paper [Song et al., 2020a]:

$$x_{t-1}(\hat{x}_0, \epsilon_\theta, \varepsilon) = \sqrt{\bar{\alpha}_{t-1}}\hat{x}_0 + \sqrt{1 - \bar{\alpha}_{t-1} - \sigma_t^2}\epsilon_\theta + \sigma_t\varepsilon \quad (11)$$

$$\Leftrightarrow x_{t-1}(x_t, \epsilon_\theta, \varepsilon) = \sqrt{\bar{\alpha}_{t-1}}\left(\frac{x_t - \sqrt{1 - \bar{\alpha}_t}\epsilon_\theta}{\sqrt{\alpha_t}}\right) + \sqrt{1 - \bar{\alpha}_{t-1} - \sigma_t^2}\epsilon_\theta + \sigma_t\varepsilon \quad (12)$$

with $\hat{x}_0 = \frac{x_t - \sqrt{1 - \bar{\alpha}_t}\epsilon_\theta(x_t, t)}{\sqrt{\alpha_t}}$ as the prediction of x_0 given (x_t, t) . The equivalence of Eq. (9) and above equations can be proved easily as follows. We have,

$$\begin{aligned} \sqrt{1 - \bar{\alpha}_{t-1} - \sigma_t^2} &= \sqrt{1 - \bar{\alpha}_{t-1} - \frac{1 - \bar{\alpha}_{t-1}}{1 - \bar{\alpha}_t}(1 - \alpha_t)} \\ &= (1 - \bar{\alpha}_{t-1})\sqrt{\frac{\alpha_t}{1 - \bar{\alpha}_t}} \end{aligned}$$

Therefore, with Eq. (11),

$$\begin{aligned} x_{t-1}(\hat{x}_0, \epsilon_\theta, \varepsilon) &= \sqrt{\bar{\alpha}_{t-1}}\hat{x}_0 + \sqrt{1 - \bar{\alpha}_{t-1} - \sigma_t^2}\epsilon_\theta + \sigma_t\varepsilon \\ &= \sqrt{\bar{\alpha}_{t-1}}\hat{x}_0 + \sqrt{1 - \bar{\alpha}_{t-1} - \sigma_t^2}\epsilon_\theta + \sigma_t\varepsilon \\ &= \sqrt{\bar{\alpha}_{t-1}}\hat{x}_0 + (1 - \bar{\alpha}_{t-1})\sqrt{\frac{\alpha_t}{1 - \bar{\alpha}_t}}\frac{x_t - \sqrt{\bar{\alpha}_t}\hat{x}_0}{\sqrt{1 - \bar{\alpha}_t}} + \sigma_t\varepsilon \\ \Leftrightarrow x_{t-1}(\hat{x}_0, x_t, \varepsilon) &= \frac{\sqrt{\bar{\alpha}_{t-1}}(1 - \alpha_t)}{1 - \bar{\alpha}_t}\hat{x}_0 + \frac{\sqrt{\alpha_t}(1 - \bar{\alpha}_{t-1})}{1 - \bar{\alpha}_t}x_t + \sigma_t\varepsilon \end{aligned}$$

Therefore, equivalence of Eq. (11) and Eq. (10) is proved.

From Eq. (11), another form of x_{t-1} is as following:

$$\begin{aligned}
x_{t-1}(\hat{x}_0, \epsilon_\theta, \varepsilon) &= \sqrt{\bar{\alpha}_{t-1}}\hat{x}_0 + \sqrt{1 - \bar{\alpha}_{t-1} - \sigma_t^2}\epsilon_\theta + \sigma_t\varepsilon \\
&= \sqrt{\bar{\alpha}_{t-1}}\hat{x}_0 + \sqrt{1 - \bar{\alpha}_{t-1} - \sigma_t^2}\left(\frac{1}{\sqrt{1 - \bar{\alpha}_t}}x_t - \frac{\sqrt{\bar{\alpha}_t}}{\sqrt{1 - \bar{\alpha}_t}}\hat{x}_0\right) + \sigma_t\varepsilon \\
\Leftrightarrow x_{t-1}(x_t, \hat{x}_0, \varepsilon) &= \left(\sqrt{\bar{\alpha}_{t-1}} - \sqrt{1 - \bar{\alpha}_{t-1} - \sigma_t^2}\frac{\sqrt{\bar{\alpha}_t}}{\sqrt{1 - \bar{\alpha}_t}}\right)\hat{x}_0 + \frac{\sqrt{1 - \bar{\alpha}_{t-1}}}{\sqrt{1 - \bar{\alpha}_t}}x_t + \sigma_t\varepsilon
\end{aligned} \tag{13}$$

Therefore, Eq. (10), Eq. (11), Eq. (12) and Eq. (13) are all equivalent forms of Eq. (9) for deriving x_{t-1} with x_t , just with different input arguments and formats. It is common to see each representation in practical implementation.

Denoising Diffusion Implicit Model [Song et al., 2020a]. DDIM follows Eq. (12) for posterior sampling, with two additional modifications:

(i). DDIM also generalizes for arbitrary subsequence of $\{0, 1, \dots, T\}$ as:

$$\boxed{x_{t_{n-1}}(x_{t_n}, \epsilon_\theta, \varepsilon) = \sqrt{\bar{\alpha}_{t_{n-1}}}\left(\frac{x_{t_n} - \sqrt{1 - \bar{\alpha}_{t_n}}\epsilon_\theta}{\sqrt{\bar{\alpha}_{t_n}}}\right) + \sqrt{1 - \bar{\alpha}_{t_{n-1}} - \sigma_{t_n}^2}\epsilon_\theta + \sigma_{t_n}\varepsilon} \tag{14}$$

with the timestep subsequence being $\{t_0, t_1, \dots, t_N\} \subseteq \{0, 1, \dots, T\}, t_0 = 0$. Note that $\bar{\alpha}_{t_n} = \prod_{i=0}^{t_n} \alpha_i \neq \prod_{i=0}^n \alpha_{t_i}$

Why cannot we directly reverse Eq. (5) to get $x_{t-1} = \frac{x_t - \sqrt{1 - \alpha_t}\epsilon_\theta}{\sqrt{\alpha_t}}$? The reason is that it loses the noise ε added in the iterative sampling process and becomes deterministic sampling for entire denoising path, leading to only one sample in the end.

(ii). Actually DDIM generalizes σ_t in Eq. (9) to be (with additional η multiplier):

$$\sigma_t(\eta) = \eta \sqrt{\frac{(1 - \alpha_t)(1 - \bar{\alpha}_{t-1})}{1 - \bar{\alpha}_t}}$$

when $\eta = 0$ Eq. (9) becomes $x_{t-1} = \frac{1}{\sqrt{\alpha_t}}x_t - \frac{1 - \alpha_t}{\sqrt{1 - \alpha_t}\sqrt{\alpha_t}}\epsilon_\theta$. This makes DDIM to have deterministic sampling process. When $\eta = 1$ it becomes original stochastic DDPM. $\eta \in [0, 1]$ tunes the extent from deterministic to stochastic sampling.

It can be noticed that Eq. (9) with $\eta = 0$ is very close to reverse Eq. (5): $x_{t-1} = \frac{1}{\sqrt{\alpha_t}}x_t - \frac{\sqrt{1 - \alpha_t}}{\sqrt{\alpha_t}}\epsilon_\theta$. These two formulas are different because the previous formula is calculating $\mathbb{E}[x_{t-1}|x_t, x_0]$ as the conditional mean of x_{t-1} given x_t, x_0 , and the latter formula is computing x_{t-1} given x_t assuming a single step noise is ϵ_θ .

Another denoising inference example is that consistency model (introduced later in Sec. 2.3) applies Eq. (7) to directly get deterministically predicted \hat{x}_0 , but it is further made stochastic by adding noise again using forward diffusion process $x_{t_{n-1}} = \sqrt{\bar{\alpha}_{t_{n-1}}}\hat{x}_0 + \sqrt{1 - \bar{\alpha}_{t_{n-1}}}\varepsilon$, and so on so forth. The detailed inference process of the consistency model is discussed in Sec. 2.3.2. For the usage of subscript in timestep like t_n , it is because consistency model follows a continuous time schedule $\{t_n\}_{n=1}^N$, which is different from the discrete time schedule of $t \in \{0, \dots, T\}$ in the diffusion model.

Score-based Denoising Diffusion [Song et al., 2020b]. Different from above probabilistic inference on a Markov chain, score-based denoising diffusion models approach the diffusion generative process from a score-matching perspective. As outlined in the reverse SDE Eq. (3) or reverse ODE as Eq. (4), the score function $\nabla_{x_t} \log q(x_t)$ represents the gradient of the probability density in the diffusion process. This score function is utilized in the backward denoising process to generate samples from the target data distribution.

The score function for $q(x_t|x_0)$ in Eq. (6) is as following:

$$\begin{aligned} s(x_t, t) &:= \nabla_{x_t} \log q(x_t) \\ &= \mathbb{E}_{q(x_0)}[\nabla_{x_t} \log q(x_t|x_0)] \\ &= \mathbb{E}_{q(x_0)}\left[-\frac{\varepsilon}{\sqrt{1-\bar{\alpha}_t}}\right] \end{aligned} \quad (15)$$

$$= -\frac{\varepsilon}{\sqrt{1-\bar{\alpha}_t}} \quad (16)$$

$$= -\frac{x_t - \sqrt{\bar{\alpha}_t}x_0}{1-\bar{\alpha}_t} \quad (\text{By Eq. (6)}) \quad (17)$$

The Eq. (15) applies for a fixed value of random noise ε . The derivation leverages the fact that: For $x \sim p(x) = \mathcal{N}(\mu, \sigma^2\mathbf{I})$, $\nabla_x \log p(x) = \nabla_x(-\frac{1}{2\sigma^2}(x-\mu)^2) = -\frac{x-\mu}{\sigma^2} = -\frac{\varepsilon}{\sigma}$, $\varepsilon \sim \mathcal{N}(0, \mathbf{I})$. The score function can be approximated with parameterized model as $s_\theta(x_t, t) \approx s(x_t, t)$ in practice, with expression:

$$\boxed{s_\theta(x_t, t) = -\frac{\epsilon_\theta(x_t, t)}{\sqrt{1-\bar{\alpha}_t}}} \quad (18)$$

$\epsilon_\theta(x_t, t)$ is the parameterized noise prediction function with time and sample x_t as inputs.

This score function connects DDPM and score-based denoising diffusion, which will be discussed more in later sections.

Demystify notations from different papers.

DDPM uses notations as Eq. (5): $q(x_t|x_{t-1}) = \mathcal{N}(x_t; \sqrt{\alpha_t^{\text{DDPM}}}x_{t-1}, (1-\alpha_t^{\text{DDPM}})\mathbf{I})$.

DDIM [Song et al., 2020a] follows the notations of score-based denoising diffusion [Song et al., 2020b], where $q(x_t|x_0) = \mathcal{N}(x_t; \sqrt{\alpha_t^{\text{DDIM}}}x_0, (1-\alpha_t^{\text{DDIM}})\mathbf{I})$.

LCM [Luo et al., 2023] and DMD [Yin et al., 2024b] use notations $q(x_t|x_0) = \mathcal{N}(x_t; \alpha_t^{\text{LCM}}x_0, (\sigma_t^{\text{LCM}})^2\mathbf{I})$.

The connection of three sets of notations is $\bar{\alpha}^{\text{DDPM}} = \alpha^{\text{DDIM}} = (\alpha^{\text{LCM}})^2$, $\sigma^{\text{LCM}} = \sqrt{1 - (\alpha^{\text{LCM}})^2} = \sqrt{1 - \bar{\alpha}^{\text{DDPM}}}$.

This paper keeps DDPM notations, which are more consistent with code implementation.

2.2.2 Training

The training process of diffusion models centers on deriving an appropriate objective $\mathcal{L}(\theta)$, which can be derived from a variety of foundational perspectives. In most practical cases, θ represents the parameters of a neural network, optimized using standard machine learning techniques, such as supervised learning with gradient descent. This subsection examines the mathematical formulation of diffusion model training objectives, emphasizing their connections

to noise prediction and score matching, while aiming to present a unified perspective on these methodologies.

DDPM Objective for Training. We first construct the variational lower bound for $\log p_\theta(x_0)$:²

$$\begin{aligned}
-\log p_\theta(x_0) &\leq -\log p_\theta(x_0) + D_{\text{KL}}(q(x_{1:T}|x_0)||p_\theta(x_{1:T}|x_0)) \\
&= -\log p_\theta(x_0) + \mathbb{E}_{x_{1:T} \sim q(x_{1:T}|x_0)} \left[\log \frac{q(x_{1:T}|x_0)}{p_\theta(x_{0:T})/p_\theta(x_0)} \right] \\
&= -\log p_\theta(x_0) + \mathbb{E}_q \left[\log \frac{q(x_{1:T}|x_0)}{p_\theta(x_{0:T})} + \log p_\theta(x_0) \right] \\
&= \mathbb{E}_q \left[\log \frac{q(x_{1:T}|x_0)}{p_\theta(x_{0:T})} \right]
\end{aligned}$$

which is the variational lower bound of log-likelihood, following a similar derivation as variational auto-encoder [Kingma, 2013] but on a Markov chain.

Next step is to expand the lower bound for variance reduction, with details in [Sohl-Dickstein et al., 2015]:

$$\begin{aligned}
\mathcal{L}_{\text{VLB}} &= \mathbb{E}_{q(x_{0:T})} \left[\log \frac{q(x_{1:T}|x_0)}{p_\theta(x_{0:T})} \right] \\
&= \mathbb{E}_q \left[\log \frac{\prod_{t=1}^T q(x_t|x_{t-1})}{p_\theta(x_T) \prod_{t=1}^T p_\theta(x_{t-1}|x_t)} \right] \\
&= \mathbb{E}_q \left[-\log p_\theta(x_T) + \sum_{t=1}^T \log \frac{q(x_t|x_{t-1})}{p_\theta(x_{t-1}|x_t)} \right] \\
&= \mathbb{E}_q \left[-\log p_\theta(x_T) + \sum_{t=2}^T \log \frac{q(x_t|x_{t-1}, x_0)}{p_\theta(x_{t-1}|x_t)} + \log \frac{q(x_1|x_0)}{p_\theta(x_0|x_1)} \right] \\
&= \mathbb{E}_q \left[-\log p_\theta(x_T) + \sum_{t=2}^T \log \left(\frac{q(x_{t-1}|x_t, x_0)}{p_\theta(x_{t-1}|x_t)} \cdot \frac{q(x_t|x_0)}{q(x_{t-1}|x_0)} \right) + \log \frac{q(x_1|x_0)}{p_\theta(x_0|x_1)} \right] \\
&= \mathbb{E}_q \left[-\log p_\theta(x_T) + \sum_{t=2}^T \log \frac{q(x_{t-1}|x_t, x_0)}{p_\theta(x_{t-1}|x_t)} + \sum_{t=2}^T \log \frac{q(x_t|x_0)}{q(x_{t-1}|x_0)} + \log \frac{q(x_1|x_0)}{p_\theta(x_0|x_1)} \right] \\
&= \mathbb{E}_q \left[-\log p_\theta(x_T) + \sum_{t=2}^T \log \frac{q(x_{t-1}|x_t, x_0)}{p_\theta(x_{t-1}|x_t)} + \log \frac{q(x_T|x_0)}{q(x_1|x_0)} + \log \frac{q(x_1|x_0)}{p_\theta(x_0|x_1)} \right] \\
&= \mathbb{E}_q \left[\log \frac{q(x_T|x_0)}{p_\theta(x_T)} + \sum_{t=2}^T \log \frac{q(x_{t-1}|x_t, x_0)}{p_\theta(x_{t-1}|x_t)} - \log p_\theta(x_0|x_1) \right] \\
&= \mathbb{E}_q \left[\underbrace{D_{\text{KL}}(q(x_T|x_0)||p_\theta(x_T))}_{\mathcal{L}_T} + \sum_{t=2}^T \underbrace{D_{\text{KL}}(q(x_{t-1}|x_t, x_0)||p_\theta(x_{t-1}|x_t))}_{\mathcal{L}_{t-1}} - \underbrace{\log p_\theta(x_0|x_1)}_{\mathcal{L}_0} \right]
\end{aligned}$$

²This part is adopted from Lilian Weng's blog [Weng, 2021], with full credit attributed to it.

Since $x_T \sim \mathcal{N}(0, \mathbf{I})$ which is a Gaussian noise, the \mathcal{L}_T term actually does not contain θ and can be dropped. \mathcal{L}_0 is practically usually also dropped or approximated with $D_{\text{KL}}(q(x_\epsilon|x_1, x_0)||p_\theta(x_\epsilon|x_1))$ with a sufficiently small ϵ close to zero. Then the entire loss \mathcal{L}_{VLB} becomes a sum of KL-divergence between Gaussians, which can be analytically calculated as:

$$\begin{aligned} \mathcal{L}_t &= \mathbb{E}_{x_0, \epsilon_t} \left[\frac{1}{2\|\Sigma_\theta(x_t, t)\|_2^2} \|\mu_t(x_t, x_0) - \mu_\theta(x_t, t)\|_2^2 \right] \\ &= \mathbb{E}_{x_0, \epsilon_t} \left[\frac{1}{2\|\Sigma_\theta\|_2^2} \left\| \frac{1}{\sqrt{\alpha_t}} \left(x_t - \frac{1 - \alpha_t}{\sqrt{1 - \bar{\alpha}_t}} \epsilon_t \right) - \frac{1}{\sqrt{\alpha_t}} \left(x_t - \frac{1 - \alpha_t}{\sqrt{1 - \bar{\alpha}_t}} \epsilon_\theta(x_t, t) \right) \right\|_2^2 \right] \\ &= \mathbb{E}_{x_0, \epsilon_t} \left[\frac{(1 - \alpha_t)^2}{2\alpha_t(1 - \bar{\alpha}_t)\|\Sigma_\theta\|_2^2} \|\epsilon_t - \epsilon_\theta(x_t, t)\|_2^2 \right] \\ &= \mathbb{E}_{x_0, \epsilon_t} \left[\frac{(1 - \alpha_t)^2}{2\alpha_t(1 - \bar{\alpha}_t)\|\Sigma_\theta\|_2^2} \|\epsilon_t - \epsilon_\theta(\sqrt{\bar{\alpha}_t}x_0 + \sqrt{1 - \bar{\alpha}_t}\epsilon_t, t)\|_2^2 \right] \end{aligned}$$

by choosing parameterization,

$$\mu_\theta(x_t, t) = \frac{1}{\sqrt{\alpha_t}} x_t - \frac{1 - \alpha_t}{\sqrt{1 - \bar{\alpha}_t} \sqrt{\alpha_t}} \epsilon_\theta$$

Score Matching Objective for Training. We first answer the question:

Why using score matching?

Score matching originates from 2005 by [Hyvärinen and Dayan, 2005]. Given the ground-truth sample distribution $q(x)$, the objective is to learn the parameterized probability density model p_θ as:

$$p(x; \theta) = \frac{1}{Z(\theta)} \exp(-E(x; \theta))$$

where the partition function $Z(\theta) = \int_{x \in \mathbb{R}^d} \exp(-E(x; \theta))$ is generally intractable. Score matching is to bypass the estimation of $Z(\theta)$ in above probability density estimation process.

Specifically, the score function is the gradient of the log-density with respect to sample vector as:

$$\psi(x; \theta) = \begin{pmatrix} \frac{\partial \log p(x; \theta)}{\partial x_1} \\ \vdots \\ \frac{\partial \log p(x; \theta)}{\partial x_d} \end{pmatrix} = \begin{pmatrix} \psi_1(x; \theta) \\ \vdots \\ \psi_d(x; \theta) \end{pmatrix} = \nabla_x \log p(x; \theta)$$

which is not dependent on $Z(\theta)$, and this is the critical property for us to leverage the score matching method.

For score matching, two equivalent objectives have been derived: Explicit Score Matching (ESM) and Implicit Score Matching (ISM), as named later by [Vincent, 2011].

The objectives are:

$$J_{\text{ESM}_q}(\theta) = \mathbb{E}_{q(x)} \left[\frac{1}{2} \left\| \psi(x; \theta) - \frac{\partial \log q(x)}{\partial x} \right\|_2^2 \right]$$

$$\begin{aligned}
J_{ISM_q}(\theta) &= \mathbb{E}_{q(\mathbf{x})} \left[\frac{1}{2} \|\psi(x; \theta)\|_2^2 + \nabla_x \cdot \psi(x; \theta) \right] \quad (\nabla_x \cdot () \text{ as divergence}) \\
&= \mathbb{E}_{q(\mathbf{x})} \left[\frac{1}{2} \|\psi(x; \theta)\|_2^2 + \sum_{i=1}^d \frac{\partial \psi_i(x; \theta)}{\partial x_i} \right] \\
&= \mathbb{E}_{q(\mathbf{x})} \left[\frac{1}{2} \|\psi(x; \theta)\|_2^2 + \text{Tr}(\nabla_x \psi(x; \theta)) \right]
\end{aligned}$$

where $\nabla_x \cdot \psi(x; \theta) = \text{Tr}(\nabla_x \psi(x; \theta))$ as $\psi : \mathbb{R}^d \rightarrow \mathbb{R}^d$ is a vector field.

We have equivalence of ESM and ISM:

$$J_{ESM_q}(\theta) = J_{ISM_q}(\theta) + C$$

where C is a constant independent on θ .

Score-based denoising diffusion [Song and Ermon, 2019, Song et al., 2020b] applies ESM objective generalized for $t \in [T]$, where the score function $\nabla_{x_t} \log q(x_t)$ can be estimated with neural networks s_θ :

$$\begin{aligned}
\mathcal{L}_{SM} &= \int_0^T w(t) \mathbb{E}_{x_t \sim q(x_t)} [\|\nabla_{x_t} \log q(x_t) - s_\theta(x_t, t)\|_2^2] dt \\
&\approx \mathbb{E}_{t \in [0, T], x_t \sim q(x_t)} [w(t) \|\nabla_{x_t} \log q(x_t) - s_\theta(x_t, t)\|_2^2] \quad (\text{time discretization}) \\
&= \mathbb{E}_{t \in [0, T], x_t \sim q(x_t)} [w(t) \left\| -\frac{x_t - \sqrt{\bar{\alpha}_t} x_0}{1 - \bar{\alpha}_t} + \frac{\epsilon_\theta(x_t, t)}{\sqrt{1 - \bar{\alpha}_t}} \right\|_2^2] \quad (\text{by Eq. (17) and (18)}) \\
&= \mathbb{E}_{x_0 \sim q(x_0), t \in [0, T], \epsilon \sim \mathcal{N}(0, \mathbf{I})} \left[\frac{w(t)}{\sqrt{1 - \bar{\alpha}_t}} \|\epsilon_\theta(x_t, t) - \epsilon\|_2^2 \right] \quad (\text{By Eq. (6)})
\end{aligned}$$

with $x_t = \sqrt{\bar{\alpha}_t} x_0 + \sqrt{1 - \bar{\alpha}_t} \epsilon$, $\epsilon \sim \mathcal{N}(0, \mathbf{I})$. ϵ_θ is the parameterized noise prediction model for ϵ -prediction. Other forms of prediction are discussed in Sec. 2.6. This matches the loss used in DDPM regardless of the time-dependent coefficients.

The naive choice of $w(t) = 1$ and constant t leads to that the score matching norm is estimated on the sample distribution $\mathbb{E}_{x_t \sim q(x_t)} [\|\nabla_x \log q(x_t) - s_\theta(x_t)\|_2^2]$, which causes inaccurate score estimation for low density regions in the sample space. There is also the trade-off of the noise scale (depending on t) added to x_t , that smaller noise leads to lower coverage of low density regions and less corruption of data distribution, while larger noise leads to higher coverage of low density regions and more corruption of the data distribution.

Later improvement applies multi-scale noise perturbation with noise-conditional score network (NCSN) [Song and Ermon, 2019, Song and Ermon, 2020] $s_\theta(x_t, t)$ to solve this issue, with the loss expression shown in above \mathcal{L}_{SM} equation. $w(t)$ is typically chosen to be $w(t) \propto 1/\mathbb{E}[\|\nabla_{x_t} \log q(x_t|x_0)\|_2^2]$ for loss balancing over time. For example, it can be set as $w(t) = \sigma_t^2$.

(Approximate) equivalence of objectives.

Regardless of the coefficients, the score matching objective coincides with the DDPM objective as the mean-squared-error (MSE) of noise prediction. In practice, the coefficients in front of MSE are usually dropped for simplicity.

2.2.3 Inference

After training, the diffusion models are applied for the denoising function in an iterative manner to generate diverse yet accurate prediction of \hat{x}_0 , which is referred to as the inference process. We describe three types of sampling process for diffusion model inference.

(1). DDPM Sampling: The inference process of DDPM (for ϵ -prediction model) requires iteratively: (i). predicting noise $\epsilon_\theta(x_t, t)$, starting with Gaussian noise $x_T \sim \mathcal{N}(0, \mathbf{I})$; (ii). derive \hat{x}_0 using ϵ_θ with $\hat{x}_0 = \frac{1}{\sqrt{\bar{\alpha}_t}}x_t - \frac{\sqrt{1-\bar{\alpha}_t}}{\sqrt{\bar{\alpha}_t}}\epsilon_\theta$ by Eq. (7); (iii). $x_{t-1}(x_t, \hat{x}_0, \epsilon) = \frac{\sqrt{\bar{\alpha}_{t-1}(1-\alpha_t)}}{1-\bar{\alpha}_t}\hat{x}_0 + \frac{\sqrt{\bar{\alpha}_t(1-\bar{\alpha}_{t-1})}}{1-\bar{\alpha}_t}x_t + \sigma_t\epsilon$ by Eq. (10). This iterative process is executed along the entire diffusion timestep sequence $[T]$ for original DDPM sampling. Compared with few-step sampling, the multi-step iterative denoising and diffusion process increases the diversity and fidelity of generated samples. The procedure for DDPM inference is shown in Alg. 1. Practically, there exists a simpler sampling method for DDPM inference as Alg. 2, which no longer requires estimation of posterior mean and variance. The Alg. 2 as a simpler form cannot be used to estimate the probability of samples due to lack of mean and standard deviation for the distribution. For both algorithms, it employs the ϵ -prediction as in most practical usage, where the parameterized models directly approximate the noise ϵ_θ . Other forms of prediction parameterization can be applied with appropriate variable transformations, as discussed in detail in later Sec. 2.6

(2). DDIM Sampling: Instead of conducting denoising along the entire diffusion process that can be computationally expensive at inference time, DDIM or stratified sampling allows to sample along a sub-set $\{t_n\}_{n=1}^N \subseteq [T]$ for inference acceleration.

The DDIM sampling follows Eq. (14), by replacing the x_{t-1} -prediction formula in DDPM inference step (iii) with the following:

$$x_{t_{n-1}}(x_{t_n}, \epsilon_\theta, \epsilon) = \sqrt{\bar{\alpha}_{t_{n-1}}} \left(\frac{x_{t_n} - \sqrt{1 - \bar{\alpha}_{t_n}} \epsilon_\theta}{\sqrt{\bar{\alpha}_{t_n}}} \right) + \sqrt{1 - \bar{\alpha}_{t_{n-1}} - \sigma_{t_n}^2} \epsilon_\theta + \sigma_{t_n} \epsilon$$

for any subsequence $\{t_0, t_1, \dots, t_N\} \subseteq [T]$, $t_0 = 0$.

A side-by-side comparison of DDPM and DDIM inference is displayed as Alg. 1 and Alg. 3. It may be noticed that DDIM uses Eq. (14) instead of Eq. (10) in DDPM as posterior mean prediction, although the two equations are previously proved to be equivalent. The two equations behave differently when the inference is performed on a subsequence $\{t_n\}_{n=1}^N \subseteq [T]$ in DDIM. For example, when $t-1 = t_{n-1} = 0$, $\bar{\alpha}_{t-1} = \bar{\alpha}_{t_{n-1}} = 1$, Eq. (14) gives $\mu = \hat{x}_0$ while Eq. (10) gives $\mu = \frac{(1-\alpha_t)\sqrt{\bar{\alpha}_t}}{1-\bar{\alpha}_t}\hat{x}_0$, which is wrong. This indicates that Eq. (10) cannot be applied on a subsequence of $[T]$ as in DDIM. The procedure for DDIM inference is shown in Alg. 3, with ϵ -prediction explained above.

(3). SMLD Sampling: Score matching is used for learning the score function, and Langevin dynamics is used for sampling at inference time. The joint usage is called score matching Langevin dynamics (SMLD) [Song and Ermon, 2019]. After learning the score function, new samples can be generated using Langevin dynamics, which is derived by the iterative update rule:

$$x_{t+1} = x_t + \frac{\delta}{2} s_\theta(x_t) + \sqrt{\delta} \epsilon_t$$

where:

- x_0 is sampled from Gaussian distribution;

- δ is the step size;
- $s_\theta(x_t)$ is the learned score function;
- $\varepsilon_t \sim \mathcal{N}(0, \mathbf{I})$ is Gaussian noise.

Here it follows the original update rules as presented in [Song and Ermon, 2019], where the process begins with a random Gaussian x_0 and progresses towards x_T , representing the target distribution. This approach is equivalent to the formulation in DDPM by a change of variable $x_t \rightarrow x_{T-t}$. In this framework, the denoising process proceeds with increasing t , with the sample distribution being derived as $T \rightarrow \infty$. This process iteratively refines the sample x_t with the learned score and incorporating Gaussian noise to ensure adequate exploration. In the limit of step size approaching zero, the process converges to samples from the true distribution through Langevin dynamics.

Algorithm 1 DDPM inference with ϵ -prediction

- 1: $x_T \sim \mathcal{N}(0, \mathbf{I})$
 - 2: **for** $t \in [T]$ **do**
 - 3: predict noise $\epsilon_\theta(x_t, t)$
 - 4: $\hat{x}_0 \leftarrow \frac{1}{\sqrt{\alpha_t}} x_t - \frac{\sqrt{1-\alpha_t}}{\sqrt{\alpha_t}} \epsilon_\theta$ by Eq. (7)
 - 5: $\mu_\theta(x_{t-1}) \leftarrow \frac{(1-\alpha_t)\sqrt{\alpha_t}}{1-\alpha_t} \hat{x}_0 + \frac{\sqrt{\alpha_t}(1-\bar{\alpha}_{t-1})}{1-\alpha_t} x_t$ as Eq. (10)
 - 6: $\sigma_t \leftarrow \sqrt{(1-\alpha_t) \frac{1-\bar{\alpha}_{t-1}}{1-\alpha_t}}$
 - 7: $x_{t-1} \leftarrow \mu_\theta + \sigma_t \cdot \varepsilon, \varepsilon \sim \mathcal{N}(0, \mathbf{I})$
 - 8: **end for**
-

Algorithm 2 DDPM inference with ϵ -prediction (simplified)

- 1: $x_T \sim \mathcal{N}(0, \mathbf{I})$
 - 2: **for** $t \in [T]$ **do**
 - 3: predict noise $\epsilon_\theta(x_t, t)$
 - 4: $x_{t-1} \leftarrow \frac{1}{\sqrt{\alpha_t}} (x_t - \frac{1-\alpha_t}{\sqrt{1-\alpha_t}} \epsilon_\theta) + \sqrt{1-\bar{\alpha}_{t-1}} \varepsilon, \varepsilon \sim \mathcal{N}(0, \mathbf{I})$ as Eq. (9)
 - 5: **end for**
-

Algorithm 3 DDIM inference with ϵ -prediction

- 1: $x_{t_N} \sim \mathcal{N}(0, \mathbf{I}), \{t_n\}_{n=1}^N \subseteq [T]$
 - 2: **for** $n \in [N]$ **do**
 - 3: predict noise $\epsilon_\theta(x_{t_n}, t_n)$
 - 4: $\hat{x}_0 \leftarrow \frac{1}{\sqrt{\alpha_{t_n}}} x_{t_n} - \frac{\sqrt{1-\alpha_{t_n}}}{\sqrt{\alpha_{t_n}}} \epsilon_\theta$ by Eq. (7)
 - 5: $\mu_\theta(x_{t_{n-1}}) \leftarrow \sqrt{\alpha_{t_{n-1}}} \hat{x}_0 + \sqrt{1-\bar{\alpha}_{t_{n-1}} - \sigma_{t_n}^2} \epsilon_\theta$ as Eq. (14)
 - 6: $\sigma_{t_n} \leftarrow \eta \sqrt{(1-\alpha_{t_n}) \frac{1-\bar{\alpha}_{t_{n-1}}}{1-\alpha_{t_n}}}$
 - 7: $x_{t_{n-1}} \leftarrow \mu_\theta + \sigma_{t_n} \cdot \varepsilon, \varepsilon \sim \mathcal{N}(0, \mathbf{I})$
 - 8: **end for**
-

2.3 Consistency Model

The diffusion model [Ho et al., 2020, Song et al., 2020b] solves the multi-modal distribution matching problem with a stochastic differential equation (SDE), while the consistency model [Song et al., 2023] solves an equivalent probability flow ordinary differential equation

(ODE):

$$\frac{dx_t}{dt} = -t\nabla \log p_t(x)$$

with $p_t(x) = p_{\text{data}}(x) \otimes \mathcal{N}(0, t^2\mathbf{I})$ for time period $t \in [0, T]$, where $p_{\text{data}}(x)$ is the data distribution. The reverse process along the solution trajectory $\{\hat{x}_\tau\}_{\tau \in [\epsilon, T]}$ of this ODE is the data generation process from initial random samples $\hat{x}_T \sim \mathcal{N}(0, T^2\mathbf{I})$, with ϵ as a small constant close to 0 for handling numerical problem at the boundary. Specifically, it approximates a parameterized consistency function $f_\theta : (x_t, t) \rightarrow x_\epsilon$, which is defined as a map from the noisy sample x_t at step t back to the original sample x_ϵ , instead of applying a step-by-step denoising function $p_\theta(x_{t-1}|x_t)$ as the reverse diffusion process in diffusion model.

2.3.1 Training

The parameterized consistency model f_θ is enforced to satisfy the boundary condition:

$$f_\theta(x_t, t) = c_{\text{skip}}(t)x_t + c_{\text{out}}(t)x_\theta(x_t, c, t) \quad (19)$$

where $c_{\text{skip}}(t) = \frac{\sigma^2}{(t-\epsilon)^2 + \sigma^2}$ and $c_{\text{out}}(t) = \frac{\sigma(t-\epsilon)}{\sqrt{t^2 + \sigma^2}}$, as a boundary condition satisfying $f_\theta(x_\epsilon, \epsilon) = x_\epsilon \approx x_0$ when $\epsilon \rightarrow 0$. In practice the data standard deviation takes $\sigma = 0.5$, small constant $\epsilon = 0.002$ (practically usually using t_{-1} for indexing as a trick)³.

The training process of a consistency model can be achieved with (i). consistency distillation with a ODE solver or (ii). consistency training without the solver.

Consistency Distillation. The consistency distillation loss is defined as the $\lambda(t_n)$ -weighted distance of two model predictions:

$$\begin{aligned} \mathcal{L}_{\text{CD}}(\theta) &= \mathbb{E}[\lambda(t_n)d(f_\theta(x_{t_{n+1}}, t_{n+1}), f_{\theta^-}(\hat{x}_{t_n}, t_n))] \\ \hat{x}_{t_n} &= \text{Denoise}(x_{t_{n+1}}, t_{n+1}, t_n) \end{aligned} \quad (20)$$

where $\lambda(t_n)$ is a time dependent coefficient usually set as constant in practice, and $d(\cdot, \cdot)$ is a distance metric like l_2 loss $d(x, y) = \|x - y\|_2^2$, Pseudo-Huber loss $d(x, y) = \sqrt{\|x - y\|_2^2 + c^2} - c$ with $c > 0$ [Song and Dhariwal, 2023], or LPIPS loss [Zhang et al., 2018]. $\text{Denoise}(x_{t_{n+1}}, t_{n+1}, t_n)$ is the denoising function (*e.g.*, an ODE solver) to denoise samples from t_{n+1} to t_n . In the distillation setting, the denoising function can be implemented with a pre-trained teacher diffusion model. For example, by using pretrained diffusion noise prediction ϵ_ϕ , based on DDIM sampling as Eq. (14):

$$\text{Denoise}(x_{t_{n+1}}, t_{n+1}, t_n; \epsilon_\phi) := \sqrt{\bar{\alpha}_{t_n}} \left(\frac{x_{t_{n+1}} - \sqrt{1 - \bar{\alpha}_{t_{n+1}}} \epsilon_\phi}{\sqrt{\bar{\alpha}_{t_{n+1}}}} \right) + \sqrt{1 - \bar{\alpha}_{t_n} - \sigma_{t_{n+1}}^2} \epsilon_\phi + \sigma_{t_{n+1}} \epsilon \quad (21)$$

ϕ is used for ϵ_ϕ here to distinguish from learnable θ . $\sigma_{t_{n+1}} = 0$ for DDIM sampler.

Option1: multi-step denoising function. It also allows to conduct m -step denoising as:

$$\hat{x}_{t_n} = \text{Denoise}^m(x_{t_{n+m}}, t_{n+m}, t_n)$$

³Append 0.002 to get time sequence $\{t_1, \dots, t_n, \dots, t_N, 0.002\}$, and retrieve value 0.002 with $n = -1$.

$$= \text{Denoise}(\text{Denoise}(\dots \text{Denoise}(x_{t_{n+m}}, t_{n+m}, t_n))) \quad (22)$$

with more computational cost.

Option2: CFG augmentation. It is an option to use classifier-free guidance (CFG) [Ho and Salimans, 2022] augmented prediction with given guidance weight w in the denoising function:

$$\epsilon_\phi(x_{t_{n+1}}, c, t_{n+1}, t_n, w) = \epsilon_\phi(x_{t_{n+1}}, c, t_{n+1}, t_n) + w(\epsilon_\phi(x_{t_{n+1}}, c, t_{n+1}, t_n) - \epsilon_\phi(x_{t_{n+1}}, \emptyset, t_{n+1}, t_n)) \quad (23)$$

Merging above Eq. (23) into Eq. (21) gives DDIM sample with CFG augmentation.

Reparameterization from DM to CM. Given diffusion model (DM) ϵ_θ , using Eq. (19) and (6), consistency model f_θ can be reparameterized by (proposed by LCM [Luo et al., 2023]):

$$\begin{aligned} f_\theta(x_t, t) &= c_{\text{skip}}x_t + c_{\text{out}}x_\theta(x_t, c, t) \\ x_\theta &= \frac{x_t - \sqrt{1 - \bar{\alpha}_t}\epsilon_\theta(x_t, c, t)}{\sqrt{\bar{\alpha}_t}} \end{aligned} \quad (24)$$

where x_θ is the prediction of clean sample \hat{x}_0 . Note that it also requires the DM and CM to have aligned timesteps t (at least DM timesteps need to cover CM timesteps).

Benefits of the reparameterization. In the distillation process of CM from pre-trained DM, this parameterization allows ϵ_θ to be initialized with ϵ_ϕ for achieving the minimal distillation efforts.

Discussion. Note that in LCM paper, they write an equivalent representation of Eq. (20) and (21):

$$\begin{aligned} \Psi(x_{t_{n+1}}, t_{n+1}, t_n, c) &= \sqrt{\frac{\bar{\alpha}_{t_n}}{\bar{\alpha}_{t_{n+1}}}}x_{t_{n+1}} - \sigma_{t_n} \left(\frac{\sigma_{t_{n+1}} \cdot \sqrt{\bar{\alpha}_{t_n}}}{\sqrt{\bar{\alpha}_{t_{n+1}}} \cdot \sigma_{t_n}} - 1 \right) \epsilon_\phi(x_{t_{n+1}}, c, t_{n+1}) - x_{t_{n+1}} \\ &= \sqrt{\bar{\alpha}_{t_n}} \left(\frac{x_{t_{n+1}} - \sqrt{1 - \bar{\alpha}_{t_{n+1}}}\epsilon_\phi}{\sqrt{\bar{\alpha}_{t_{n+1}}}} \right) + \sqrt{1 - \bar{\alpha}_{t_n}}\epsilon_\phi - x_{t_{n+1}} \end{aligned}$$

and

$$\begin{aligned} \hat{x}_{t_n} &= x_{t_{n+1}} + (1 + w)\Psi(x_{t_{n+1}}, t_{n+1}, t_n, c) - w\Psi(x_{t_{n+1}}, t_{n+1}, t_n, \emptyset) \\ &= \text{Denoise}(x_{t_{n+1}}, t_{n+1}, t_n; \epsilon_\phi) \end{aligned}$$

which is exactly the same as Eq. (21) when $\sigma_{t_{n+1}} = 0$.

Consistency Training. Different from above consistency distillation process, the consistency training (CT) loss is defined according to the self-consistency property without distillation from any teacher model:

$$\mathcal{L}_{\text{CT}}(\theta) = \mathbb{E}[\lambda(t_n)d(f_\theta(x_{t_{n+1}}, t_{n+1}), f_{\theta^-}(x_{t_n}, t_n))] \quad (25)$$

with $d(\cdot, \cdot)$ as a distance metric.

The following theorem presents the convergence property of CT towards CD with respect to the timestep interval.

Theorem 2.2 [Song et al., 2023] Define a maximum of timestep interval $\Delta t = \max_{n \in [N-1]} |t_{n+1} - t_n|$, under certain Lipschitz and smooth conditions, and assuming ground-truth teacher score model in CD, we have

$$\begin{aligned}\mathcal{L}_{CD}^N &= \mathcal{L}_{CT}^N + o(\Delta t) \\ \mathcal{L}_{CT}^N &\geq O(\Delta t) \text{ if } \inf \mathcal{L}_{CD}^N > 0\end{aligned}$$

where Δt can be a function of training iteration k . The first equation holds when Δt is sufficiently small due to the usage of Taylor expansion. It essentially implies that when iteration k becomes large enough and $\Delta t(k) \leq \epsilon$, if $\mathcal{L}_{CT}^N \leq \epsilon_{CT}$, then $\mathcal{L}_{CD}^N \leq \epsilon_{CT} + \epsilon$, and ϵ is much smaller than ϵ_{CT} . This is the reason why CT takes $t_n(k)$ with a decreasing scale as training iteration k increases, which tries to minimize \mathcal{L}_{CT}^N and the difference of \mathcal{L}_{CD}^N and \mathcal{L}_{CT}^N when $|t_{n+1}(k) - t_n(k)|$ becomes infinitely small in theory.

2.3.2 Inference

The inference process of consistency model involves iteratively:

1. predict $\hat{x}_0 = f_\theta(x_{t_{n+1}}, t_{n+1})$ as Eq. (19);
2. add noise with forward diffusion as Eq. (6) for timestep t_n :

$$x_{t_n} = \hat{x}_0 + \sqrt{t_n^2 - \epsilon^2} \varepsilon, \varepsilon \sim \mathcal{N}(0, \mathbf{I}) \quad (26)$$

in standard consistency model, ϵ is a small constant value close to 0 as a lower bound of time. This is a variance exploding noise schedule.

The pseudo-code for multi-step sampling with consistency models is shown in Alg. 4.

If using LCM reparameterization, it follows the same variance preserving noise schedule as DDPM:

$$x_{t_n} = \sqrt{\bar{\alpha}_{t_n}} \hat{x}_0 + \sqrt{1 - \bar{\alpha}_{t_n}} \varepsilon, \varepsilon \sim \mathcal{N}(0, \mathbf{I}) \quad (27)$$

Algorithm 4 CM inference with f -prediction

- 1: $x_{t_N} \sim \mathcal{N}(0, \mathbf{I}), \{t_n\}_{n=1}^N \subseteq [T]$
 - 2: **for** $n \in [N]$ **do**
 - 3: predict $\hat{x}_0 \leftarrow f_\theta(x_{t_n}, t_n)$
 - 4: $x_{t_{n-1}} = \hat{x}_0 + \sqrt{t_{n-1}^2 - \epsilon^2} \varepsilon, \varepsilon \sim \mathcal{N}(0, \mathbf{I})$
as Eq. (26)
 - 5: **end for**
-

Algorithm 5 LCM inference with ϵ -prediction

- 1: $x_{t_N} \sim \mathcal{N}(0, \mathbf{I}), \{t_n\}_{n=1}^N \subseteq [T]$
 - 2: **for** $n \in [N]$ **do**
 - 3: predict noise $\epsilon_\theta(x_{t_n}, t_n)$
 - 4: $\hat{x}_0 \leftarrow \frac{1}{\sqrt{\bar{\alpha}_{t_n}}} x_{t_n} - \frac{\sqrt{1 - \bar{\alpha}_{t_n}}}{\sqrt{\bar{\alpha}_{t_n}}} \epsilon_\theta$ by Tweedie
Eq. (7)
 - 5: $x_{t_{n-1}} \leftarrow \sqrt{\bar{\alpha}_{t_{n-1}}} \hat{x}_0 + \sqrt{1 - \bar{\alpha}_{t_{n-1}}} \varepsilon, \varepsilon \sim \mathcal{N}(0, \mathbf{I})$
 - 6: **end for**
-

Additionally, LCM has boundary satisfaction as $f_\theta(x_0, t_0) = x_0$ for $t_0 = \epsilon$, and:

$$\hat{x}_0 = x_\theta = \frac{x_{t_{n+1}} - \sqrt{1 - \bar{\alpha}_{t_{n+1}}}\epsilon_\theta(x_{t_{n+1}}, c, t_{n+1})}{\sqrt{\bar{\alpha}_{t_{n+1}}}}$$

Plug into Eq. (27)

$$x_{t_n} = \sqrt{\bar{\alpha}_{t_n}} \frac{x_{t_{n+1}} - \sqrt{1 - \bar{\alpha}_{t_{n+1}}}\epsilon_\theta(x_{t_{n+1}}, c, t_{n+1})}{\sqrt{\bar{\alpha}_{t_{n+1}}}} + \sqrt{1 - \bar{\alpha}_{t_{n+1}}}\epsilon, \epsilon \sim \mathcal{N}(0, \mathbf{I})$$

The pseudo-code for multi-step sampling with LCM is shown in Alg. 5. It is worth noting that the LCM sampling is exactly the same as DDIM sampling with random noise $\sigma_t = 0$ (as Eq. (14) with $\epsilon \rightarrow \epsilon_\theta$). This provides another interpretation of the relationship between consistency inference and DDIM inference as follows.

Proposition 2.3 *DDIM inference is approximately (ignoring boundary satisfaction in consistency model) the consistency inference with LCM reparameterization by just using predicted noise $\epsilon_\theta(x_{t_{n+1}}, c, t_{n+1})$ instead of random noise $\epsilon \sim \mathcal{N}(0, \mathbf{I})$ in the diffusion process from \hat{x}_0 to x_{t_n} .*

Variance Preserving and Variance Exploding Noise Schedule. Different from previously introduced DDPM with $x_t = \sqrt{\alpha_t}x_{t-1} + \sqrt{1 - \alpha_t}\epsilon, \epsilon \sim \mathcal{N}(0, \mathbf{I})$, which has preserved variance with a constant norm, the standard consistency model has exploding variance $\sigma_d^2 + t_n^2$, as indicated by noise adding formula Eq. (25). Its variance increases over the timestep, and σ_d^2 is the variance of training samples. LCM follows DDPM noise schedule as Eq. (27), therefore also preserves the variance norm even with consistency distillation.

2.4 Rectified Flow

Rectified flow [Liu et al., 2022] or flow matching [Lipman et al., 2022] is a special class of diffusion models, following certain noise schedules in general diffusion models defined as Def. 2.1. For the continuous case, it takes $\bar{a}_t = 1 - t, \bar{b}_t = t$.

2.4.1 Training

Training Objective. The rectified flow connects two arbitrary distributions $y_0 \sim \pi_0, y_1 \sim \pi_1$. In a manner similar to diffusion models or consistency models, we have $\pi_0 = q(y), \pi_1 = \mathcal{N}(0, \mathbf{I})$. The forward rectified flow process linearly interpolates y_t as:

$$y_t = ty_1 + (1 - t)y_0, t \in [0, 1].$$

We want to learn the velocity at any t : $v(y_t, t) = \frac{d}{dt}y_t = y_1 - y_0$. It is optimized through the loss:

$$v_1 = \arg \min_v \int_0^1 \mathbb{E}_{y_0 \sim \pi_0, y_1 \sim \pi_1} [|| (y_1 - y_0) - v(y_t, t) ||^2] dt, y_t = ty_1 + (1 - t)y_0. \quad (28)$$

By optimizing above Eq. (28) we derive **1-Rectified Flow** v_1 . After ideal optimization process, v_1 already achieves certain deterministic mapping for each pair of sample $y_0 \sim \pi_0$ and $y_1 \sim \pi_1$. We use it generate paired samples (y_0, y_1) for further rectifying it to get **2-Rectified Flow** v_2 , which is also called the *Reflow* process:

$$v_2 = \arg \min_v \int_0^1 \mathbb{E}_{y_0 \sim \pi_0, y_1 = \text{Flow}_1(y_0)} [|| (y_1 - y_0) - v(y_t, t) ||^2] dt, y_t = ty_1 + (1-t)y_0. \quad (29)$$

where $\text{Flow}_k(y_0) = y_0 + \int_0^1 v_k(y_t, t) dt$. This helps to find more straighter and shorter path for connecting paired (y_0, y_1) than **1-Rectified Flow** v_1 . Iteratively, it can achieve **k -Rectified Flow** with $O(1/k)$ rate of straightness of the mappings.

Distillation. The above process can also be viewed as a distillation process which helps to find straighter paths and reduces sampling steps from a pre-trained RF model. The optimization objective for RF distillation is:

$$v = \arg \min_v \mathbb{E}_{y_0 \sim \pi_0} [d(\text{Flow}_k(y_0), y_0 + v(y_0))]$$

with $d(\cdot, \cdot)$ is a distance metric. This objective is actually the same as **k -Rectified Flow**, with k being the number of iterations of *Reflow* for the distillation. This is for one-step distillation as $y_0 + v(y_0)$ is one-step inference.

2.4.2 Inference

As π_0 and π_1 are symmetric in above formulation, the inference process of rectified flow can be bidirectional: $\pi_0 \rightarrow \pi_1$ or $\pi_1 \rightarrow \pi_0$, with a simple sign transformation of velocity. For $\pi_0 \rightarrow \pi_1$, the process is straightforward by $\text{Flow}_k(y_0) = y_0 + \int_0^1 v_k(y_t, t) dt, y_0 \sim \pi_0$. For discrete timesteps $[t_0, t_1, \dots, t_N]$, $\hat{y}_{t_0} = y_{t_N} + \sum_{i=1}^N (t_i - t_{i-1}) v_k(y_{t_i}, t_i)$ with $x_{t_N} \sim \mathcal{N}(0, \mathbf{I})$. On the contrary, for $\pi_1 \rightarrow \pi_0$, which is in consistency with the practical requirement of mapping noise back to the original data distribution, this can be achieved by redefining $v = -v$ while utilizing the same sampling formulas. By default, we will use this redefined velocity $v = y_0 - y_1$ as the mapping function from noise y_1 to data sample y_0 in subsequent sections to ensure consistency.

2.4.3 InstaFlow-prediction

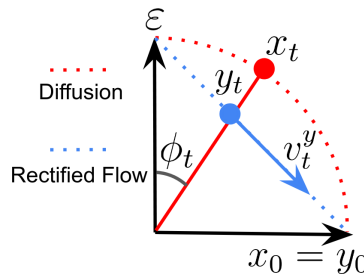


Figure 1: Relationship of v -prediction in diffusion and InstaFlow-prediction in rectified flow

The InstaFlow-prediction [Liu et al., 2023b] follows the previously introduced rectified flow (RF) method. In InstaFlow-prediction, the method works on a conjugate space $(y_t, v_\theta^y)_{t=0}^T \in$

$(\mathcal{Y} \times \mathcal{V})^T$ instead of original $(x_t, \epsilon_\theta)_{t=0}^T \in (\mathcal{X} \times \mathcal{E})^T$, with a one-to-one transformation for each x_t and y_t , $\forall t \in [T]$, and $y_0 = x_0$, as visualized in Fig. 1. We will use the upperscript to distinguish between velocity v^x along the diffusion model trajectory and velocity v^y along the RF trajectory.

The InstaFlow network (following RF) directly predicts the target velocity \tilde{v}^y along the RF trajectory, as the difference of the clean sample and Gaussian noise:

$$v_\theta^y \approx \tilde{v}^y = x_0 - \varepsilon \quad (30)$$

Since the RF sample y_t is a scaled version of diffusion sample x_t as:

$$y_t = \frac{x_t}{\sqrt{\bar{\alpha}_t} + \sqrt{1 - \bar{\alpha}_t}} = \gamma_t x_0 + (1 - \gamma_t)\varepsilon, \gamma_t = \frac{\sqrt{\bar{\alpha}_t}}{\sqrt{\bar{\alpha}_t} + \sqrt{1 - \bar{\alpha}_t}}, \quad (31)$$

which satisfies $y_0 = x_0$.

x_θ -prediction in InstaFlow. Given the InstaFlow network output v_θ^y , we can derive the prediction of original sample x_θ as:

$$\begin{aligned} \gamma_t x_\theta &= y_t - (1 - \gamma_t)(x_\theta - v_\theta^y) \\ x_\theta &= y_t + (1 - \gamma_t)v_\theta^y = y_t + \frac{\sqrt{1 - \bar{\alpha}_t}}{\sqrt{\bar{\alpha}_t} + \sqrt{1 - \bar{\alpha}_t}}v_\theta^y \\ x_\theta &= \frac{(\sqrt{\bar{\alpha}_t} + \sqrt{1 - \bar{\alpha}_t})y_t - \sqrt{1 - \bar{\alpha}_t}\varepsilon_\theta}{\sqrt{\bar{\alpha}_t}} \end{aligned} \quad (32)$$

by replacing x_0 with x_θ in Eq. (31).

ϵ_θ -prediction in InstaFlow. Given the InstaFlow network output v_θ^y , the prediction of noise ϵ_θ as:

$$\begin{aligned} (1 - \gamma_t)\epsilon_\theta &= y_t - \gamma_t(v_\theta^y + \epsilon_\theta) \\ \epsilon_\theta &= y_t - \gamma_t v_\theta^y = y_t - \frac{\sqrt{\bar{\alpha}_t}}{\sqrt{\bar{\alpha}_t} + \sqrt{1 - \bar{\alpha}_t}}v_\theta^y \end{aligned} \quad (33)$$

by replacing ε with ϵ_θ in Eq. (31).

Score estimation in InstaFlow. The score estimation follows:

$$s_\theta(x_t, t) = -\frac{x_t - \sqrt{\bar{\alpha}_t}x_\theta}{1 - \bar{\alpha}_t}, \quad x_t = y_t \cdot (\sqrt{\bar{\alpha}_t} + \sqrt{1 - \bar{\alpha}_t})$$

with the $x_t \rightarrow y_t$ transformation caused by the InstaFlow prediction. y_t follows Eq. (31) and x_θ follows Eq. (32).

Posterior distribution of x_{t-1} in InstaFlow. Original Eq. (10) for x_{t-1} prediction now becomes:

$$\begin{aligned} x_{t-1}(x_t, x_0, \varepsilon) &= \frac{\sqrt{\bar{\alpha}_{t-1}}(1 - \alpha_t)}{1 - \bar{\alpha}_t} x_\theta + \frac{\sqrt{\alpha_t}(1 - \bar{\alpha}_{t-1})}{1 - \bar{\alpha}_t} x_t + \sigma_t \varepsilon \\ \Leftrightarrow y_{t-1} \beta_{t-1} &= \frac{\sqrt{\bar{\alpha}_{t-1}}(1 - \alpha_t)}{1 - \bar{\alpha}_t} (y_t + (1 - \gamma_t) v_\theta^y) + \frac{\sqrt{\alpha_t}(1 - \bar{\alpha}_{t-1})}{1 - \bar{\alpha}_t} y_t \beta_t + \sigma_t \varepsilon \end{aligned}$$

where $\beta_t = \sqrt{\bar{\alpha}_t} + \sqrt{1 - \bar{\alpha}_t}$, $\sigma_t = \sqrt{\frac{(1 - \alpha_t)(1 - \bar{\alpha}_{t-1})}{1 - \bar{\alpha}_t}}$.

Detailed process of InstaFlow inference with v -prediction is shown in Alg. 6.

Algorithm 6 InstaFlow inference with v -prediction

- 1: $y_T \sim \mathcal{N}(0, \mathbf{I})$
 - 2: **for** $t \in [T]$ **do**
 - 3: predict velocity $v_\theta^y(y_t, t)$
 - 4: $\hat{x}_0 \leftarrow y_t + \frac{\sqrt{1 - \bar{\alpha}_t}}{\sqrt{\bar{\alpha}_t} + \sqrt{1 - \bar{\alpha}_t}} v_\theta^y$ by Eq. (32)
 - 5: $\mu_\theta(y_{t-1}) \leftarrow [\frac{(1 - \alpha_t)\sqrt{\bar{\alpha}_t}}{1 - \bar{\alpha}_t} \hat{x}_0 + \frac{\sqrt{\alpha_t}(1 - \bar{\alpha}_{t-1})}{1 - \bar{\alpha}_t} y_t \beta_t] / \beta_{t-1}$ as Eq. (10)
 - 6: $\sigma_t \leftarrow \sqrt{(1 - \alpha_t) \frac{1 - \bar{\alpha}_{t-1}}{1 - \bar{\alpha}_t}} / \beta_{t-1}$
 - 7: $y_{t-1} \leftarrow \mu_\theta + \sigma_t \cdot \varepsilon, \varepsilon \sim \mathcal{N}(0, \mathbf{I})$
 - 8: **end for**
-

Practically, there exists a simpler sampling method for InstaFlow inference as Alg. 7, which no longer requires estimation of posterior mean and variance. The disadvantage is that the simpler form cannot be used to estimate the probability of samples due to lack of mean and standard deviation for the distribution.

Algorithm 7 InstaFlow inference with v -prediction (simplified)

- 1: $y_T \sim \mathcal{N}(0, \mathbf{I})$
 - 2: **for** $t \in [T]$ **do**
 - 3: predict velocity $v_\theta^y(y_t, t)$
 - 4: $\hat{x}_0 \leftarrow y_t + \frac{\sqrt{1 - \bar{\alpha}_t}}{\sqrt{\bar{\alpha}_t} + \sqrt{1 - \bar{\alpha}_t}} v_\theta^y$ by Eq. (32)
 - 5: $y_{t-1} \leftarrow (\sqrt{\bar{\alpha}_{t-1}} \hat{x}_0 + \sqrt{1 - \bar{\alpha}_{t-1}} \varepsilon) / \beta_{t-1}, \varepsilon \sim \mathcal{N}(0, \mathbf{I})$
 - 6: **end for**
-

InstaFlow prediction with DDIM sampling. What if we use both InstaFlow v -prediction and also DDIM sampling? The inference method will be different from Alg. 6.

Specifically, as discussed previously in Sec. 2.2.3, Eq. (10) cannot be applied for DDIM sampling on subsequence. Instead, Eq. (14) should be used in DDIM sampling, with certain changes considering InstaFlow prediction:

$$\begin{aligned} \mu(x_{t_{n-1}}) &= \sqrt{\bar{\alpha}_{t_{n-1}}} \hat{x}_0 + \sqrt{1 - \bar{\alpha}_{t_{n-1}} - \sigma_{t_n}^2} \epsilon_\theta \\ \beta_{t_{n-1}} \mu(y_{t_{n-1}}) &= \sqrt{\bar{\alpha}_{t_{n-1}}} \hat{x}_0 + \sqrt{1 - \bar{\alpha}_{t_{n-1}} - \sigma_{t_n}^2} (y_{t_n} - \frac{\sqrt{\bar{\alpha}_{t_n}}}{\beta_{t_n}} v_\theta^y) \quad (\text{by Eq. (33)}) \end{aligned} \quad (34)$$

This provides algorithm for InstaFlow prediction with DDIM sampling for model inference, as Alg. 8.

Algorithm 8 InstaFlow inference with v -prediction and DDIM sampling

- 1: $y_{t_N} \sim \mathcal{N}(0, \mathbf{I}), \{t_n\}_{n=1}^N \subseteq [T]$
 - 2: **for** $n \in [N]$ **do**
 - 3: predict velocity $v_\theta^y(y_{t_n}, t_n)$
 - 4: $\hat{x}_0 \leftarrow y_{t_n} + \frac{\sqrt{1-\bar{\alpha}_{t_n}}}{\sqrt{\bar{\alpha}_{t_n} + \sqrt{1-\bar{\alpha}_{t_n}}}} v_\theta^y$ by Eq. (32)
 - 5: $\mu_\theta(y_{t_{n-1}}) \leftarrow [\sqrt{\bar{\alpha}_{t_{n-1}}} \hat{x}_0 + \sqrt{1-\bar{\alpha}_{t_{n-1}} - \sigma_{t_n}^2} (y_{t_n} - \frac{\sqrt{\bar{\alpha}_{t_n}}}{\beta_{t_n}} v_\theta^y)] / \beta_{t_{n-1}}$ as Eq. (34)
 - 6: $\sigma_{t_n} \leftarrow \sqrt{(1-\alpha_{t_n}) \frac{1-\bar{\alpha}_{t_{n-1}}}{1-\bar{\alpha}_{t_n}}} / \beta_{t_{n-1}}$
 - 7: $y_{t_{n-1}} \leftarrow \mu_\theta + \sigma_{t_n} \cdot \varepsilon, \varepsilon \sim \mathcal{N}(0, \mathbf{I})$
 - 8: **end for**
-

2.4.4 Distillation

In this section, we explore the possibilities of applying the rectified flow (RF) training objective in the distillation process from a diffusion model, different from the distillation from RF model itself in Sec. 2.4.1.

To leverage the loss of rectified flow in distillation from a diffusion model, there are two potential approaches: 1. learning a separate RF network for velocity prediction on RF trajectories; 2. reparameterize RF v -prediction with diffusion ϵ -prediction.

Approach 1. Take the pre-trained ϵ -prediction model ϵ_ϕ to generate paired samples (ε, \hat{x}_0) , where $\hat{x}_0 = \text{Denoise}^N(\varepsilon; \epsilon_\phi) = \text{Denoise}(\text{Denoise} \dots \text{Denoise}(\varepsilon; \epsilon_\phi))$ as defined by Eq. (22) given teacher model denoising function with N -step DDIM sampling schedule. Then take the training loss of 2-Rectified Flow as Eq. (29) to learn an individual $v(\theta)$, which is not reparameterized from ϵ_θ by v -prediction. The distillation process follows the loss:

$$\min_{\theta} \int_0^1 \mathbb{E}_{\varepsilon \sim \mathcal{N}(0, \mathbf{I}), \hat{x}_0 = \text{Denoise}^N(\varepsilon; \epsilon_\phi)} [|\hat{x}_0 - \varepsilon - v_\theta^y(x_t, t)|^2] dt, \quad (35)$$

with $x_t = tx_0 + (1-t)\varepsilon$. This essentially treats the pre-trained diffusion model with DDIM scheduler as 1-rectified flow.

Approach 2. It can be ill-posed to directly enforce rectified flow loss for student model ϵ_θ (reparameterize it into v_θ^x) in the distillation process:

$$\min_{\theta} \int_0^1 \mathbb{E}_{\varepsilon \sim \mathcal{N}(0, \mathbf{I}), \hat{x}_0 = \text{Denoise}^N(\varepsilon; \epsilon_\phi)} [|(x_0 - \varepsilon) - v_\theta^x(t)|^2] dt, \quad (36)$$

with $v_\theta^x(t) = \sqrt{1-\bar{\alpha}_t} x_\theta(x_{t'}, t') - \sqrt{\bar{\alpha}_t} \varepsilon$ representing v -prediction/parameterization in diffusion and $x_{t'} = \sqrt{\bar{\alpha}_{t'}} x_0 + \sqrt{1-\bar{\alpha}_{t'}} \varepsilon$, it becomes evident that DDIM/DDPM flows follow a circular trajectory with a constant norm, whereas RF flows along a straight line with a varying norm, as illustrated in Fig. 2. As a result, the velocity cannot be directly matched. Here, $v_\theta^x(t)$ refers to the v -prediction of the diffusion model, which characterizes the velocity along the diffusion

trajectory, rather than the v -prediction $v_\theta^y(t)$ along the RF trajectory. Given the difference in noise schedules, a mapping is required to align the velocity from the diffusion trajectory with the RF trajectory.

2.4.5 Velocity Mapping

We emphasize the relationship between velocities on the diffusion trajectory and the rectified flow trajectory. To correctly apply above Approach 2 for RF, we need to map the velocity on the diffusion trajectory $v_\theta^x(t)$ with the velocity on the RF trajectory $v_\theta^y(t)$, as demonstrated in Fig. 2 for a vector representation of the variables.

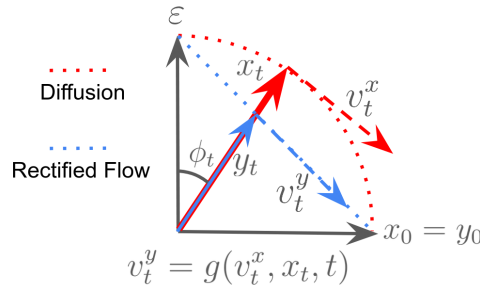


Figure 2: Velocity mapping from v -prediction in diffusion to InstaFlow-prediction in rectified flow

In Sec. 2.6.3, we prove that there exists a velocity mapping between rectified flow velocity v_t^y and diffusion velocity v_t^x :

$$v_t^y = \frac{v_t^x b - x_t(\sqrt{1 - \bar{\alpha}_t} - \sqrt{\bar{\alpha}_t})}{b^2}$$

also

$$v_t^y = \frac{x_0 - \varepsilon}{1 + 2\sqrt{\bar{\alpha}_t}\sqrt{1 - \bar{\alpha}_t}} = (x_0 - \varepsilon) \frac{\|y_t\|^2}{\|x_t\|^2}$$

which can be leveraged to form the rectified loss:

$$v_2 = \min_v \int_0^1 \mathbb{E}_{\varepsilon \sim \mathcal{N}(0, \mathbf{I}), x_0 = \text{Denoise}(\varepsilon)} [|(1 + 2\sqrt{\bar{\alpha}_t}\sqrt{1 - \bar{\alpha}_t})v_\theta^y(t) - (x_0 - \varepsilon)|^2] dt,$$

with,

$$\begin{aligned} v_\theta^y(t) &= \frac{v_t^x b_t - x_t(\sqrt{1 - \bar{\alpha}_t} - \sqrt{\bar{\alpha}_t})}{b_t^2} \\ &= \frac{(\sqrt{1 - \bar{\alpha}_t} x_\theta(t, t) - \sqrt{\bar{\alpha}_t} \varepsilon) b_t - x_t(\sqrt{1 - \bar{\alpha}_t} - \sqrt{\bar{\alpha}_t})}{b_t^2} \end{aligned}$$

$$\begin{aligned} (1 + 2\sqrt{\bar{\alpha}_t}\sqrt{1 - \bar{\alpha}_t})v_\theta^y(t) - (x_0 - \varepsilon) &= [\sqrt{\bar{\alpha}_t}(1 - \bar{\alpha}_t) + (1 - \bar{\alpha}_t)](x_\theta - x_0) \\ &= [(1 - \bar{\alpha}_t)(\sqrt{\bar{\alpha}_t} + \sqrt{1 - \bar{\alpha}_t})](\varepsilon - \varepsilon_\theta) \end{aligned}$$

with $x_\theta = \frac{1}{\sqrt{\alpha_t}}x_t - \frac{\sqrt{1-\alpha_t}}{\sqrt{\alpha_t}}\epsilon_\theta$, which is essentially a weighted regression or diffusion loss. This loss can be utilized to directly fine-tune the original diffusion model ϵ_θ (via x_θ) by enforcing the rectified flow loss on its mapped velocity, transitioning from the diffusion trajectory to the RF trajectory.

After training, the method additionally supports RF-based sampling. By transforming the diffusion velocity into RF velocity, it enables direct sampling along a straight RF trajectory, thereby facilitating efficient and effective few-step sampling.

The above discussion offers a unified perspective on the diffusion model and the RF model, integrating both their training objectives and inference processes through the mapping of velocities between the diffusion and RF processes. The next section will introduce TrigFlow, a novel model formulation designed to unify the consistency model and the RF model.

2.5 TrigFlow

TrigFlow [Lu and Song, 2024] modifies the trigonometric interpolant [Albergo and Vandenberg, 2022] to unify continuous-time consistency models and rectified flow with v prediction.

2.5.1 Training

Recall in Sec. 2.3.1, the consistency model follows EDM parameterization [Karras et al., 2022] to satisfy the boundary condition ($f_\theta(x_\epsilon, \epsilon) = x_\epsilon \approx x_0$ when $\epsilon \rightarrow 0$):

$$f_\theta(x_t, t) = c_{\text{skip}}(t)x_t + c_{\text{out}}(t)x_\theta(c_{\text{in}}(t)x_t, c_{\text{noise}}(t), c) \quad (37)$$

where $c_{\text{skip}}(t) = \frac{\sigma^2}{(t-\epsilon)^2 + \sigma^2}$, $c_{\text{out}}(t) = \frac{\sigma(t-\epsilon)}{\sqrt{t^2 + \sigma^2}}$, $c_{\text{in}}(t) = \frac{1}{\sqrt{t^2 + \sigma^2}}$ and $c_{\text{noise}}(t)$ is a transformation of t for time conditioning, σ is the standard deviation of training sample distribution. TrigFlow takes a different set of coefficients with the boundary condition also satisfied:

$$f_\theta(x_t, t) = \cos(t)x_t - \sin(t)\sigma v_\theta\left(\frac{x_t}{\sigma}, c_{\text{noise}}(t), c\right) \quad (38)$$

where v_θ is the normalized (by σ) velocity prediction with target v_t . TrigFlow can be trained using either the diffusion objective or the consistency training objective, effectively unifying the principles of rectified flow and consistency models. When employing the diffusion training objective, TrigFlow adopts velocity prediction, akin to rectified flow:

$$\mathcal{L}_{\text{TF-diffusion}} = \mathbb{E}_{x_0, \epsilon, t} [\|\sigma v_\theta\left(\frac{x_t}{\sigma}, c_{\text{noise}}(t), c\right) - v_t\|_2^2]$$

$v_t = \cos(t)\epsilon - \sin(t)x_0$ is the velocity for diffusion process $x_t = \cos(t)x_0 + \sin(t)\epsilon$, $t \in [0, \frac{\pi}{2}]$, $\epsilon \sim \mathcal{N}(0, \sigma^2\mathbf{I})$. The angular parameterization of diffusion process will be discussed later in Sec. 2.6.2. The choice of coefficients c_{skip} , c_{out} and c_{in} ensures the input of v_θ and its target to have unit variance, for the convenience of training.

Recall the discrete-time consistency training (CT) objective defined in Eq. (25). In the continuous-time setting, as $\Delta t \rightarrow 0$, its gradient is proven to converge to the following form:

$$\nabla_\theta \mathcal{L}_{\text{TF-CT}} = \nabla_\theta \mathbb{E}_{x_t, t} [\lambda(t) f_\theta^\top(x_t, t) \frac{df_{\theta^-}(x_t, t)}{dt}]$$

for l_2 distance metric $d(x, y) = \|x - y\|_2^2$.

With Eq. (38) plugged in, we have the gradients:

$$\nabla_{\theta} \mathbb{E}_{x_t, t} \left[-\lambda(t) \sin(t) \sigma v_{\theta}^{\top} \left(\frac{x_t}{\sigma}, c_{\text{noise}}(t), c \right) \frac{df_{\theta^-}(x_t, t)}{dt} \right]$$

as $\cos(t)x_t$ in $f_{\theta}(x_t, t)$ does not depend on θ .

Additional techniques are proposed to improve the training with this objective gradient in original paper [Lu and Song, 2024].

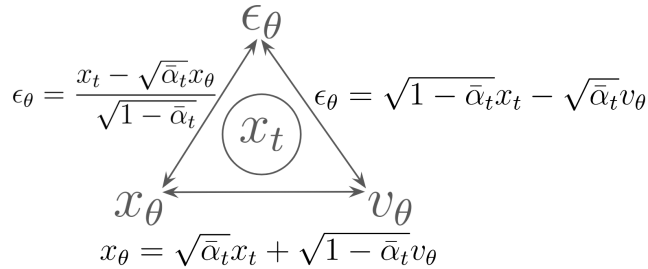
2.5.2 Inference

After training, TrigFlow model can be sampled with DDIM schedule as:

$$x_t = \cos(s - t)x_s - \sin(s - t)\sigma v_{\theta} \left(\frac{x_s}{\sigma}, c_{\text{noise}}(s), c \right)$$

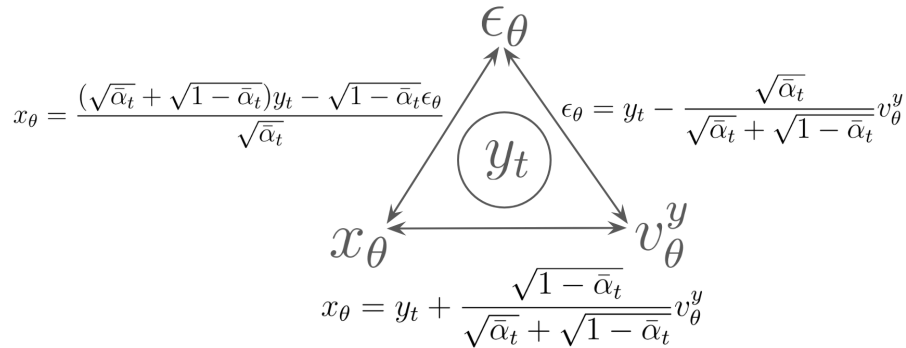
for a single step denoising from timestep s to t ($s > t$), starting from Gaussian noise $x_T \sim \mathcal{N}(0, \mathbf{I})$, $T = \frac{\pi}{2}$.

2.6 Prediction Parameterization



$$\begin{aligned} \epsilon_{\theta} &= \frac{x_t - \sqrt{\bar{\alpha}_t} x_{\theta}}{\sqrt{1 - \bar{\alpha}_t}} & \epsilon_{\theta} &= \sqrt{1 - \bar{\alpha}_t} x_t - \sqrt{\bar{\alpha}_t} v_{\theta} \\ x_{\theta} &= \sqrt{\bar{\alpha}_t} x_t + \sqrt{1 - \bar{\alpha}_t} v_{\theta} \end{aligned}$$

Figure 3: The “triangular”-formula in diffusion model for three parameterization: ϵ -prediction, x -prediction and v -prediction.



$$\begin{aligned} x_{\theta} &= \frac{(\sqrt{\bar{\alpha}_t} + \sqrt{1 - \bar{\alpha}_t}) y_t - \sqrt{1 - \bar{\alpha}_t} \epsilon_{\theta}}{\sqrt{\bar{\alpha}_t}} & \epsilon_{\theta} &= y_t - \frac{\sqrt{\bar{\alpha}_t}}{\sqrt{\bar{\alpha}_t} + \sqrt{1 - \bar{\alpha}_t}} v_{\theta}^y \\ x_{\theta} &= y_t + \frac{\sqrt{1 - \bar{\alpha}_t}}{\sqrt{\bar{\alpha}_t} + \sqrt{1 - \bar{\alpha}_t}} v_{\theta}^y \end{aligned}$$

Figure 4: The “triangular”-formula in rectified flow model for three parameterization: ϵ -prediction, x -prediction and v -prediction.

In this section, we discuss different prediction parameterizations for various models, including diffusion model, consistency model and rectified flow. The relationship among different parameterizations connect these models, which is useful for practical transformation from one type of model to another.

For diffusion model, we have the “triangular”-formula for three parameterization: ϵ -prediction, x -prediction and v -prediction, as Fig. 3.

For rectified flow model, we have the “triangular”-formula for three parameterization: ϵ -prediction, x -prediction and v -prediction, as Fig. 4.

2.6.1 ϵ -prediction and x -prediction in Diffusion Model

According to Tweedie’s formula, the ϵ -prediction and x -prediction can be mutually transformed via:

$$\epsilon_\theta = \frac{x_t - \sqrt{\bar{\alpha}_t}x_\theta}{\sigma_t}$$

$$x_\theta = \frac{x_t - \sigma_t\epsilon_\theta}{\sqrt{\bar{\alpha}_t}}$$

with $\sigma_t = \sqrt{1 - \bar{\alpha}_t}$.

Based on the “triangular”-formula relationship, we show a diagram of ϵ -prediction loss and x -prediction loss for diffusion model as in Fig. 5 and Fig. 6.

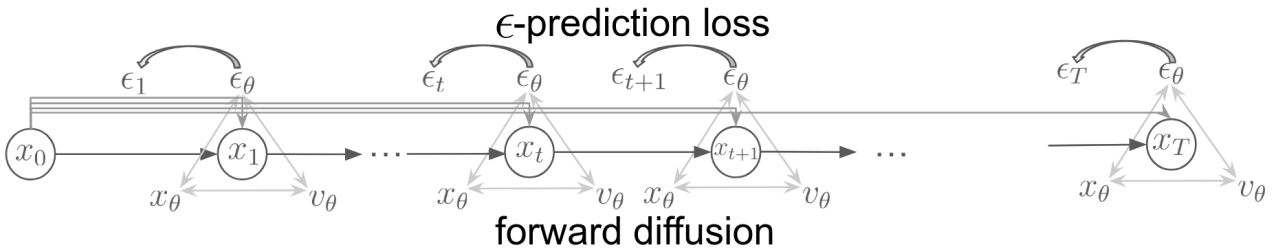


Figure 5: ϵ -prediction loss along the diffusion trajectory.

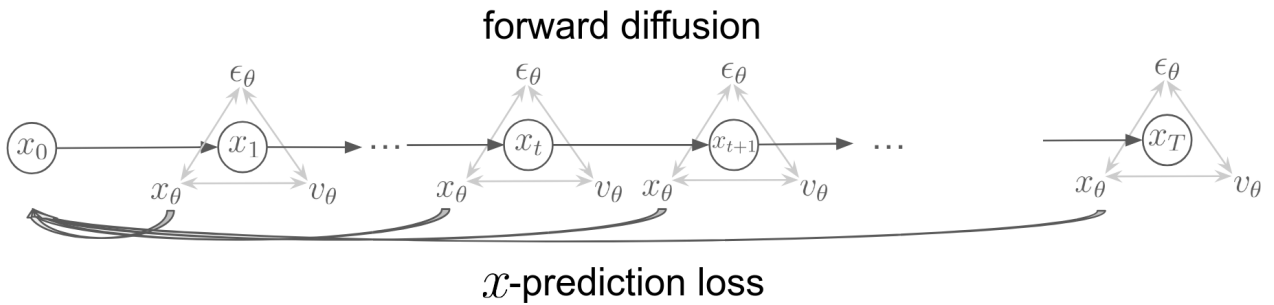


Figure 6: x -prediction loss along the diffusion trajectory.



Figure 7: Visualization of v -prediction (left) and reverse \bar{v} -prediction (right) in diffusion process.

2.6.2 v -prediction in Diffusion Model

Apart from ϵ -prediction, there is also a commonly used v -prediction. Eq. (6) can be rewritten in angular coordinate as:

$$x_t = x_0 \sin \phi_t + \epsilon \cos \phi_t$$

where $\sin \phi_t = \sqrt{\bar{\alpha}_t}$, $\cos \phi_t = \sqrt{1 - \bar{\alpha}_t}$. Then angular velocity $v_t = \frac{dx_t}{dt} = \cos \phi_t x_0 - \sin \phi_t \epsilon$ for reverse diffusion. Velocity for forward diffusion is just $\bar{v}_t = -\frac{dx_t}{dt} = -\cos \phi_t x_0 + \sin \phi_t \epsilon = -\sqrt{1 - \bar{\alpha}_t} x_0 + \sqrt{\bar{\alpha}_t} \epsilon$. Therefore the v -prediction (for reverse diffusion by default) is:

$$v_\theta = \sqrt{1 - \bar{\alpha}_t} x_\theta - \sqrt{\bar{\alpha}_t} \epsilon_\theta$$

and we have its connection to ϵ - and x -prediction:

$$\begin{aligned} x_\theta &= \sqrt{\bar{\alpha}_t} x_t + \sqrt{1 - \bar{\alpha}_t} v_\theta \\ \epsilon_\theta &= \sqrt{1 - \bar{\alpha}_t} x_t - \sqrt{\bar{\alpha}_t} v_\theta \\ \Rightarrow \epsilon_\theta &= \frac{x_t}{\sqrt{1 - \bar{\alpha}_t}} - \frac{\sqrt{\bar{\alpha}_t} x_\theta}{\sqrt{1 - \bar{\alpha}_t}} \end{aligned}$$

The Fig. 7 illustrates the v -prediction in diffusion process.

Here we intentionally choose the direction of velocity to coincide with the direction of velocity in rectified flow.

Note that practically people sometimes use v -prediction for forward diffusion velocity: $\bar{v}_\theta = \sqrt{\bar{\alpha}_t} \epsilon_\theta - \sqrt{1 - \bar{\alpha}_t} x_\theta$, which satisfies:

$$\begin{aligned} x_\theta &= \sqrt{\bar{\alpha}_t} x_t - \sqrt{1 - \bar{\alpha}_t} \bar{v}_\theta \\ \epsilon_\theta &= \sqrt{1 - \bar{\alpha}_t} x_t + \sqrt{\bar{\alpha}_t} \bar{v}_\theta \\ \Rightarrow \epsilon_\theta &= \frac{x_t}{\sqrt{1 - \bar{\alpha}_t}} - \frac{\sqrt{\bar{\alpha}_t} x_\theta}{\sqrt{1 - \bar{\alpha}_t}} \end{aligned}$$

which corresponds to Fig. 7 right image. At inference, this just requires to reverse the sign of velocity for sampling from ϵ to x_0 .

2.6.3 v -prediction in Rectified Flow

Notice that the v -prediction above (denoted as v_t^x) is along the diffusion trajectory, therefore it is different from the RF's velocity prediction (as Eq. (30)) along the RF trajectory denoted

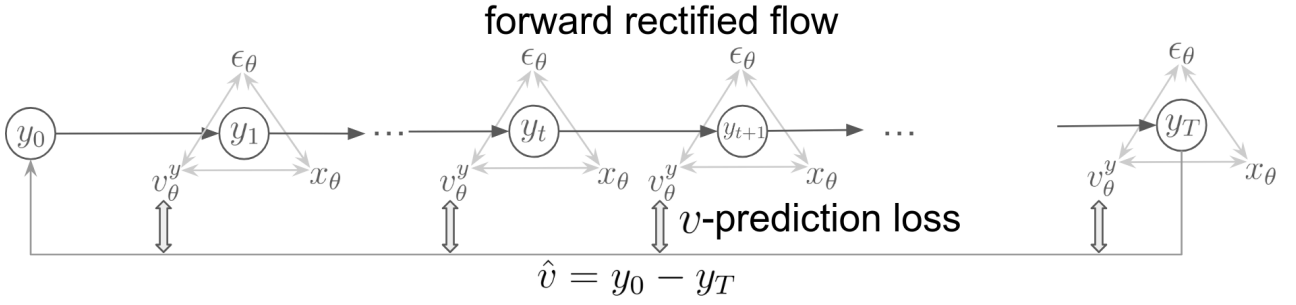


Figure 8: v -prediction loss along the RF trajectory.

as v_t^y . We also call it InstaFlow-prediction. The diagram of v -prediction loss for training the RF model is shown as Fig. 8

Actually, there exists a mapping relationship between the two velocities:

$$v_t^y = \frac{v_t^x b - x_t(\sqrt{1 - \bar{\alpha}_t} - \sqrt{\bar{\alpha}_t})}{b^2}, b = \sqrt{\bar{\alpha}_t} + \sqrt{1 - \bar{\alpha}_t}$$

with the proof as following.

Proof: Suppose the sample from diffusion model is x_t and sample from rectified flow is y_t (as scaled x_t), we have

$$\begin{aligned}
 x_t &= \sqrt{\bar{\alpha}_t}x_0 + \sqrt{1 - \bar{\alpha}_t}\varepsilon \\
 y_t &= \frac{x_t}{\sqrt{\bar{\alpha}_t} + \sqrt{1 - \bar{\alpha}_t}} = \gamma_t x_0 + (1 - \gamma_t)\varepsilon, \gamma_t = \frac{\sqrt{\bar{\alpha}_t}}{\sqrt{\bar{\alpha}_t} + \sqrt{1 - \bar{\alpha}_t}} \\
 v_t^x &= \dot{x}_t = \sqrt{1 - \bar{\alpha}_t}x_0 - \sqrt{\bar{\alpha}_t}\varepsilon \\
 v_t^y &= \dot{y}_t = \frac{a'b - b'a}{b^2}, a = x_t, b = \sqrt{\bar{\alpha}_t} + \sqrt{1 - \bar{\alpha}_t} \\
 &= \frac{\dot{x}_t b - x_t(\sqrt{1 - \bar{\alpha}_t} - \sqrt{\bar{\alpha}_t})}{b^2} \\
 &= \frac{(\sqrt{1 - \bar{\alpha}_t}x_0 - \sqrt{\bar{\alpha}_t}\varepsilon)(\sqrt{\bar{\alpha}_t} + \sqrt{1 - \bar{\alpha}_t}) - (\sqrt{\bar{\alpha}_t}x_0 + \sqrt{1 - \bar{\alpha}_t}\varepsilon)(\sqrt{1 - \bar{\alpha}_t} - \sqrt{\bar{\alpha}_t})}{1 + 2\sqrt{\bar{\alpha}_t}\sqrt{1 - \bar{\alpha}_t}} \\
 &= \frac{x_0 - \varepsilon}{1 + 2\sqrt{\bar{\alpha}_t}\sqrt{1 - \bar{\alpha}_t}} \\
 &= (x_0 - \varepsilon) \frac{\|y_t\|^2}{\|x_t\|^2}
 \end{aligned} \tag{39}$$

Eq. (39) provides the velocity mapping relationship between rectified flow velocity v_t^y and diffusion velocity v_t^x . \square

For a clearer intuitive understanding, Fig. 2 illustrates the relationship of v -prediction in diffusion and InstaFlow-prediction in rectified flow.

2.6.4 ϵ -prediction and x -prediction in Rectified Flow

As illustrated in Fig. 4, there also exist at least three parameterization for RF: ϵ -prediction, x -prediction and v -prediction. Their relationships follow:

$$\begin{aligned}\epsilon_\theta &= y_t - \frac{\sqrt{\bar{\alpha}_t}}{\sqrt{\bar{\alpha}_t} + \sqrt{1 - \bar{\alpha}_t}} v_\theta^y \\ x_\theta &= \frac{(\sqrt{\bar{\alpha}_t} + \sqrt{1 - \bar{\alpha}_t})y_t - \sqrt{1 - \bar{\alpha}_t}\epsilon_\theta}{\sqrt{\bar{\alpha}_t}} \\ x_\theta &= y_t + \frac{\sqrt{1 - \bar{\alpha}_t}}{\sqrt{\bar{\alpha}_t} + \sqrt{1 - \bar{\alpha}_t}} v_\theta^y\end{aligned}$$

The three equations are mutually consistent.

2.6.5 f -prediction in Consistency Model

Given diffusion model (DM) ϵ_θ , using Eq. (19) and (6), consistency model f_θ can be reparameterized by (proposed by LCM [Luo et al., 2023]):

$$\begin{aligned}f_\theta(x_t, t) &= c_{\text{skip}}x_t + c_{\text{out}}x_\theta(x_t, c, t) \\ x_\theta &= \frac{x_t - \sqrt{1 - \bar{\alpha}_t}\epsilon_\theta(x_t, c, t)}{\sqrt{\bar{\alpha}_t}}\end{aligned}$$

where x_θ is the prediction of clean sample \hat{x}_0 . It is worth noting that this requires the DM and CM to have aligned timesteps t ; at least, the DM timesteps need to encompass the CM timesteps.

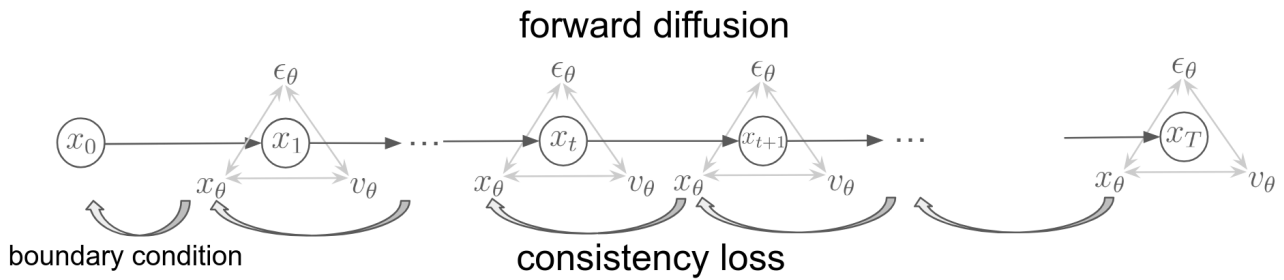


Figure 9: Consistency loss along the diffusion trajectory.

Based on the “triangular”-formula relationship, we show a diagram of consistency loss in Fig. 9.

2.7 Unified Formulation

For general SDEs connecting two arbitrary distributions $x_0 \sim \pi_0, x_1 \sim \mathcal{N}(0, \mathbf{I})$, with given sequence of coefficients $\alpha_t, \beta_t, \forall t \in [0, 1]$ (corresponding to $\bar{a}_t = \alpha_t, \bar{b}_t = \beta_t, T = 1$ in Def. 2.1):

$$x_t = \alpha_t x_0 + \beta_t x_1$$

We have the following velocity and score relationship:

$$s(x_t, t) = -\frac{x_t - \alpha_t x_0}{\beta_t^2} = -\frac{x_1}{\beta_t} \quad (\text{only for } x_1 \sim \mathcal{N}(0, \mathbf{I}))$$

$$v(x_t, t) = \frac{\dot{\alpha}_t}{\alpha_t} x_t + \beta_t \left(\frac{\dot{\alpha}_t}{\alpha_t} \beta_t - \dot{\beta}_t \right) s(x_t, t)$$

with score function $s(x_t, t) = \nabla \log p_t(x_t)$. $\dot{\alpha}_t = \frac{d\alpha_t}{dt}$, $\dot{\beta}_t = \frac{d\beta}{dt}$ as time derivatives.

Proof: Given the stochastic process:

$$x_t = \alpha_t x_0 + \beta_t x_1,$$

where $x_0 \sim \pi_0$, $x_1 \sim \pi_1$, and α_t, β_t are differentiable functions of time $t \in [0, 1]$.

The score function is defined as:

$$s(x_t, t) = \nabla_{x_t} \log p_t(x_t),$$

where $p_t(x_t)$ is the probability density function of x_t .

Since x_t is a linear transformation of x_1 given x_0 , the conditional density is:

$$p_t(x_t | x_0) = \frac{1}{\beta_t} p_{x_1} \left(\frac{x_t - \alpha_t x_0}{\beta_t} \right).$$

Compute the score function conditioned on x_0 :

$$\begin{aligned} s(x_t, t) &= \nabla_{x_t} \log p_t(x_t | x_0) \\ &= \nabla_{x_t} \log \left[\frac{1}{\beta_t} p_{x_1} \left(\frac{x_t - \alpha_t x_0}{\beta_t} \right) \right] \\ &= \nabla_{x_t} \left(-\log \beta_t + \log p_{x_1} \left(\frac{x_t - \alpha_t x_0}{\beta_t} \right) \right) \\ &= \frac{1}{\beta_t} \nabla_{x_1} \log p_{x_1}(x_1) \Big|_{x_1 = \frac{x_t - \alpha_t x_0}{\beta_t}}. \end{aligned}$$

Since $x_1 \sim \mathcal{N}(0, \mathbf{I})$, the score function of x_1 is:

$$\begin{aligned} s_{x_1}(x_1) &= \nabla_{x_1} \left(-\frac{1}{2} (x_1 - \mu)^\top \Sigma^{-1} (x_1 - \mu) \right) \\ &= -\Sigma^{-1} (x_1 - \mu) \\ &= -x_1 \end{aligned}$$

with $\mu = 0$, $\Sigma = \mathbf{I}$. Therefore:

$$s(x_t, t) = -\frac{x_t - \alpha_t x_0}{\beta_t^2} = -\frac{x_1}{\beta_t}.$$

Compute the time derivative of x_t :

$$\frac{dx_t}{dt} = \dot{\alpha}_t x_0 + \dot{\beta}_t x_1,$$

where $\dot{\alpha}_t = \frac{d\alpha_t}{dt}$ and $\dot{\beta}_t = \frac{d\beta_t}{dt}$.

Express x_0 and x_1 in terms of x_t and $s(x_t, t)$:

$$\begin{aligned} x_1 &= -\beta_t s(x_t, t), \\ x_0 &= \frac{x_t + \beta_t^2 s(x_t, t)}{\alpha_t}. \end{aligned}$$

Substitute back into $\frac{dx_t}{dt}$:

$$\begin{aligned} \frac{dx_t}{dt} &= \dot{\alpha}_t \left(\frac{x_t + \beta_t^2 s(x_t, t)}{\alpha_t} \right) + \dot{\beta}_t (-\beta_t s(x_t, t)) \\ &= \frac{\dot{\alpha}_t}{\alpha_t} x_t + \dot{\alpha}_t \left(\frac{\beta_t^2}{\alpha_t} s(x_t, t) \right) - \dot{\beta}_t \beta_t s(x_t, t). \end{aligned}$$

Simplify the coefficients:

$$\dot{\alpha}_t \left(\frac{\beta_t^2}{\alpha_t} \right) - \dot{\beta}_t \beta_t = \beta_t \left(\frac{\dot{\alpha}_t \beta_t}{\alpha_t} - \dot{\beta}_t \right).$$

Therefore, the velocity is:

$$v(x_t, t) = \frac{dx_t}{dt} = \frac{\dot{\alpha}_t}{\alpha_t} x_t + \beta_t \left(\frac{\dot{\alpha}_t \beta_t}{\alpha_t} - \dot{\beta}_t \right) s(x_t, t).$$

□

3 Diffusion Generation

Diffusion models have broad applications in modeling diverse data distributions. Leveraging neural network approximations, these models require substantial amounts of data to enhance their performance. In this section, we first present the pre-training process for various diffusion models discussed in previous sections. Next, we explore methods for diffusion model distillation to enhance inference efficiency. Finally, we outline several approaches for reward-based fine-tuning of these models.

3.1 Pre-training

In Section 2, we provided detailed introductions to various diffusion models, including the derivation of their training objectives. Here, we present a concise summary of these training objectives in a unified manner for clarity. For more details on each training objective, please refer to the corresponding sections.

3.1.1 Diffusion Model

ϵ -prediction Diffusion Model. The canonical diffusion model ϵ_θ with ϵ -prediction follows the standard objective (omitting coefficients):

$$\mathcal{L}_{\text{DM}} = \mathbb{E}_{x_0 \sim q(x_0), t \in [T], \epsilon \sim \mathcal{N}(0, \mathbf{I})} [\|\epsilon_\theta(x_t, t) - \epsilon\|_2^2]$$

Recall the x_t is a sample with diffusion noise as defined in Eq. (5).

Latent diffusion model [Rombach et al., 2022] applies a straightforward method by adding condition variable $c \in \mathcal{C}$ as input argument for conditional generation:

$$\mathcal{L}_{\text{LDM}} = \mathbb{E}_{x_0 \sim q(x_0), c, t \in [T], \varepsilon \sim \mathcal{N}(0, \mathbf{I})} [|\epsilon_\theta(x_t, c, t) - \varepsilon|_2^2]$$

with x being the latent variables after encoding. The conditional variable is usually also encoded by a text encoder like T5 or CLIP in practice.

v -prediction Diffusion Model. Alternatively, the diffusion model v_θ can predict the velocity, known as the v -prediction, with the objective:

$$\mathcal{L}_{\text{DM-v}} = \mathbb{E}_{x_0 \sim q(x_0), t \in [T], \varepsilon \sim \mathcal{N}(0, \mathbf{I})} [|\mathbf{v}_\theta(x_t, t) - v_t|_2^2]$$

with $v_\theta = \sqrt{1 - \bar{\alpha}_t} x_\theta - \sqrt{\bar{\alpha}_t} \varepsilon_\theta$, as introduced in Sec. 2.6.2. This is found to be practically more stable than ε -prediction during training in practice [Salimans and Ho, 2022].

3.1.2 Consistency Model

As introduced in Sec. 2.3.1, the consistency training objective for consistency models f_θ follows:

$$\mathcal{L}_{\text{CT}}(\theta) = \mathbb{E}[\lambda(t_n) d(f_\theta(x_{t_{n+1}}, t_{n+1}), f_{\theta^-}(x_{t_n}, t_n))]$$

with $d(\cdot, \cdot)$ as a distance metric and $t_n \in [0, T]$ following a continuous time sequence.

3.1.3 Rectified Flow

Following previous Sec. 2.4, the training objective of rectified flow (RF) model v_θ is:

$$\begin{aligned} \mathcal{L}_{\text{RF}} &= \mathbb{E}_{t \in [0, 1], x_0 \sim q(x_0)} [|\mathbf{v}_\theta(y_t, t) - v_t|_2^2] \\ v_t &= y_1 - y_0 \\ y_1 &= x_0 \\ y_0 &= \varepsilon, \varepsilon \sim \mathcal{N}(0, \mathbf{I}) \end{aligned}$$

In practice, time t is clipped to minimal value like $\sigma_{\min} = 10^{-5}$, and $y_t = ty_1 + (1 - (1 - \sigma_{\min})t)y_0$, $t \in [0, 1]$, therefore target velocity is estimated with $v_t = y_1 - (1 - \sigma_{\min})y_0$, as in Movie Gen [Polyak et al., 2024].

Rectified flow is also referred to as flow matching [Lipman et al., 2022] in literature.

3.1.4 TrigFlow

As introduced in Sec. 2.5.1, the TrigFlow model v_θ has both diffusion training and consistency training objective. The diffusion loss objective follows:

$$\mathcal{L}_{\text{TF-diffusion}} = \mathbb{E}_{x_0, \varepsilon, t} [|\sigma v_\theta(\frac{x_t}{\sigma}, c_{\text{noise}}(t), c) - v_t|_2^2]$$

with velocity $v_t = \cos(t)\varepsilon - \sin(t)x_0$ for diffusion process.

The consistency training objective has gradients:

$$\nabla_\theta \mathcal{L}_{\text{TF-CT}} = \nabla_\theta \mathbb{E}_{x_t, t} [-\lambda(t) \sin(t) \sigma v_\theta(\frac{x_t}{\sigma}, c_{\text{noise}}(t), c) \frac{df_{\theta^-}(x_t, t)}{dt}]$$

with continuous-time $t \in [0, \frac{\pi}{2}]$.

3.2 Distillation

Vanilla diffusion models typically require a large number of sampling steps through iterative denoising, often ranging from dozens to hundreds of steps in practice, especially for high-dimensional data. Beyond improved model formulations, such as consistency models, rectified flow, or TrigFlow, various techniques exist for distilling these models into versions with fewer sampling steps. This distillation process enhances sampling efficiency while maintaining comparable model performance. In this section, we introduce several such distillation methods.

3.2.1 Progressive Distillation

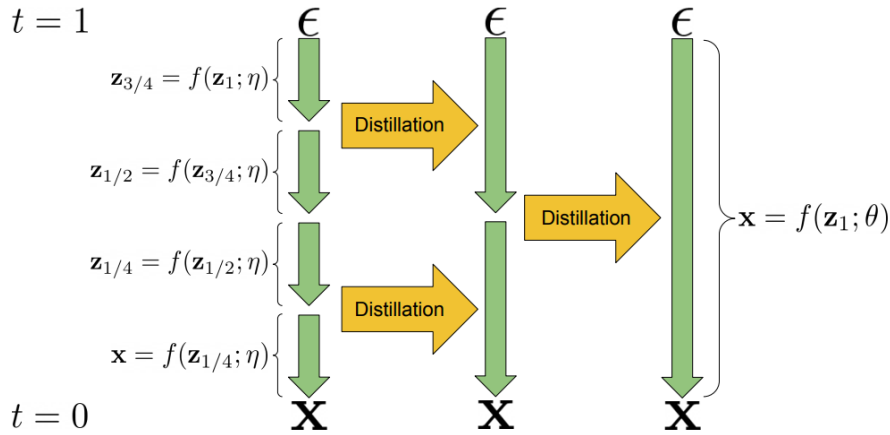


Figure 10: Overview of progressive distillation. Figure is adapted from [Salimans and Ho, 2022].

As illustrated in Fig. 10, **Progressive Distillation** (PD) [Salimans and Ho, 2022] iteratively halves the sampling steps of a teacher model and distill it into a student model. For example, for a teacher model trained on time sequence $\{t_n\}, n \in \{0, 0.5, 1, \dots, N-1, N-0.5, N\}$, the student will follow time sequence $\{t_n\}, n \in \{0, 1, \dots, N\}$. Following Eq. (14), we define a single DDIM step as:

$$x_{t_{n-1}}(x_{t_n}, \epsilon_\theta, \varepsilon) = \sqrt{\bar{\alpha}_{t_{n-1}}} \left(\frac{x_{t_n} - \sqrt{1 - \bar{\alpha}_{t_n}} \epsilon_\theta}{\sqrt{\bar{\alpha}_{t_n}}} \right) + \sqrt{1 - \bar{\alpha}_{t_{n-1}} - \sigma_{t_n}^2} \epsilon_\theta + \sigma_{t_n} \varepsilon \quad (40)$$

$$\triangleq \text{DDIM}(x_{t_n}, \epsilon_\theta)$$

To distill from a teacher model $\epsilon_{\theta'}$ with $2N$ steps, one iteration of PD will distill it into a student model ϵ_θ with N steps. Specifically, the loss function is

$$\mathcal{L}_{\text{PD}}(\theta) = \mathbb{E}_{i \in [N]} \|\tilde{x}_{t_{i-1}} - \hat{x}_{t_{i-1}}\|^2$$

with,

$$\tilde{x}_{t_{i-0.5}} = \text{DDIM}(x_{t_i}, \epsilon_{\theta'})$$

$$\tilde{x}_{t_{i-1}} = \text{DDIM}(x_{t_{i-0.5}}, \epsilon_{\theta'})$$

$$\hat{x}_{t_{i-1}} = \text{DDIM}(x_{t_i}, \epsilon_\theta)$$

The process matches the student’s one-step denoising prediction with the teacher’s two-step denoising prediction. In each iteration, the student model from the current step serves as the teacher for the next distillation iteration. After M iterations of the PD process, the student achieves a sampling process with $\lceil \frac{N}{2M} \rceil$ steps.

Guided-PD [Meng et al., 2023] extends the progressive distillation (PD) process by incorporating classifier-free guidance (CFG) from the teacher, enabling conditional generation. Specifically, the teacher leverages CFG during the distillation process. Recall Eq. (23) for the CFG-augmented prediction with guidance weight w :

$$\epsilon_\theta(x_{t_{n+1}}, c, t_{n+1}, t_n, w) = \epsilon_\theta(x_{t_{n+1}}, c, t_{n+1}, t_n) + w(\epsilon_\theta(x_{t_{n+1}}, c, t_{n+1}, t_n) - \epsilon_\theta(x_{t_{n+1}}, \emptyset, t_{n+1}, t_n))$$

Replacing it into Eq. (40) gives one-step DDIM inference with CFG: $\text{DDIM}^{\text{CFG}}(x_{t_n}, \epsilon_\theta, c, w)$ with conditional variable $c \in \mathcal{C}$. Practical guidance weight applies a constant value or a value uniformly sampled from a pre-specified range. The rest of Guided-PD follows standard PD.

3.2.2 Score Distillation Sampling

Following the previously introduced score matching objective in Sec. 2.2.2, there is a series of work for model distillation via score matching.

DreamFusion [Poole et al., 2022] introduces Score Distillation Sampling (SDS) for maximum likelihood estimation in 3D generation. The objective for SDS is to minimize the KL-divergence of parameterized noised sample distribution $p_t^\theta(x_t|c)$ at timestep t along the forward diffusion process and the real data distribution $q_t(x_t|c)$ for $\forall t \in [0.02T, 0.98T]$:

$$\mathcal{L}_{\text{SDS}} = \mathbb{E}_{t,c,\varepsilon \sim \mathcal{N}(0,\mathbf{I})} [D_{\text{KL}}(p_t^\theta(x_t|c) || q_t(x_t|c))]$$

T is the time horizon of the diffusion process (e.g., 1 for continuous timesteps or 1000 for discrete timesteps). The timestep is clipped because the score estimation can be unstable at the time boundaries, especially when $t \rightarrow 0$.

The gradient of \mathcal{L}_{SDS} is,

$$\begin{aligned} \nabla_\theta \mathcal{L}_{\text{SDS}} &= \mathbb{E}_{t,c,\varepsilon \sim \mathcal{N}(0,\mathbf{I})} [w(t) (\nabla_{x_t} \log p_t^\theta(x_t|c) - \nabla_{x_t} \log q_t(x_t|c)) \nabla_\theta G_\theta(\varepsilon, c)] \\ &= \mathbb{E}_{t,c,\varepsilon \sim \mathcal{N}(0,\mathbf{I})} [w(t) \left(-\frac{\epsilon_\theta}{\sqrt{1 - \bar{\alpha}_t}} - \left(-\frac{\varepsilon}{\sqrt{1 - \bar{\alpha}_t}} \right) \right) \nabla_\theta G_\theta(\varepsilon, c)] \end{aligned}$$

by applying the score estimation Eq. (18) in DDPM schedule.

3.2.3 Variational Score Distillation

ProlificDreamer [Wang et al., 2024c] proposes Variational Score Distillation (VSD) for 3D generation with diffusion models, as a generalized version of SDS. As pointed out in the paper, SDS often suffers from oversaturation, over-smoothing, and low-diversity issues.

Considering a parameterized generator $G_\theta(c)$, with its parameters sample from distribution $\mu(\theta)$, suppose the ground truth real data sample from $q(x_0|c)$ with c being conditions, the variational score distillation (VSD) solves the following variational inference problem,

$$\mu^* = \min_{\mu} D_{\text{KL}}(p_0^\mu(x_0|c) || q_0(x_0|c))$$

For a complex data distribution q_0 , this can be hard to optimized. However, it can be easier to optimize the problem for the distribution $q_t(x_t|c)$ of diffused sample x_t with larger t via a diffusion process. Thus, VSD construct an alternative objective for optimization with KL-divergence of denoising distributions over all timesteps,

$$\mu^* = \min_{\mu} \mathbb{E}_{t,c} \left[\frac{1}{\sqrt{\alpha_t}} w(t) D_{\text{KL}}(p_t^\mu(x_t|c) || q_t(x_t|c)) \right] \quad (41)$$

by leveraging the diffusion probability $q(x_t|x_0)$ as Eq. (6). It can be proved that Eq. (41) yields the same optimal μ^* as previous objective, with the following theorem.

Theorem 3.1 (Global optimum of VSD) For $\forall t > 0$,

$$D_{\text{KL}}(p_t^\mu(x_t|c) || q_t(x_t|c)) = 0 \Leftrightarrow p_0^\mu(x_0|c) || q_0(x_0|c)$$

The above alternative objective actually traces back to the denoising score matching [Vincent, 2011] and has been discussed in later work [Song and Ermon, 2019].

The gradient of the VSD objective is:

$$\nabla_{\theta} \mathcal{L}_{\text{VSD}} = \mathbb{E}_{t,c,\varepsilon \sim \mathcal{N}(0,\mathbf{I})} [w(t) (\nabla_{x_t} \log p_t^\mu(x_t|c) - \nabla_{x_t} \log q_t(x_t|c)) \nabla_{\theta} G_{\theta}(\varepsilon, c)]$$

with $\nabla_{\theta} x_t = \sqrt{\alpha_t} \nabla_{\theta} \hat{x}_0 = \sqrt{\alpha_t} \nabla_{\theta} G_{\theta}$, $\sqrt{\alpha_t}$ absorbed in $w(t)$. $G_{\theta}(\varepsilon, c)$ is a conditional variational generator depending on both the random noise $\varepsilon \sim \mathcal{N}(0, \mathbf{I})$ and conditional variable c . $\nabla_{x_t} \log q_t(x_t|c)$ is the real score function on noisy generated images x_t , which is estimated with a pre-trained diffusion model on real samples. $\nabla_{x_t} \log p_t^\mu(x_t|c)$ is the fake score function on noisy generated images, which is estimated with another diffusion model trained via the standard diffusion objective on generated sample distribution by G_{θ} as:

$$\mathcal{L}_{\text{diffusion}}(\phi) = \mathbb{E}_{x_0,t,\varepsilon} \|\varepsilon - \epsilon_{\phi}(F(G_{\theta}(c), t, \varepsilon))\|^2 \quad (42)$$

with $F(\cdot)$ as the forward diffusion process.

It needs to notice that the *global optimum of VSD* indicates the condition of minimal difference of scores for $\forall t > 0$ is sufficient for achieving the minimal different of scores at $t = 0$, but it does not indicate that each score can be estimated in this way individually.

More concretely, the true score can not be approximated with the expectation of diffused score estimation over diffusion timesteps and perturbation noise:

$$s(x_0) \neq \mathbb{E}_{t,x_t,\varepsilon} [s(x_t, t)] \quad (43)$$

3.2.4 Distribution Matching Distillation

As illustrated in Fig. 11, the distribution matching distillation (DMD) [Yin et al., 2024b, Yin et al., 2024a] is essentially VSD with additional generative adversarial network (GAN) loss for discriminating between the generated samples and training samples:

$$\mathcal{L}_{\text{DMD}} = \mathcal{L}_{\text{VSD}}(\theta) + \lambda_1 \mathcal{L}_{\text{diffusion}}(\phi) + \lambda_2 \mathcal{L}_{\text{adv}}(\theta, \psi)$$

DMD is employed to distill knowledge from a teacher diffusion model into a few-step student diffusion model, which, in this case, serves as the parameterized generator G_{θ} . Unlike VSD, which directly optimizes the θ -parameterized 3D generation [Wang et al., 2024c], the DMD loss optimizes an individual diffusion network for G_{θ} .

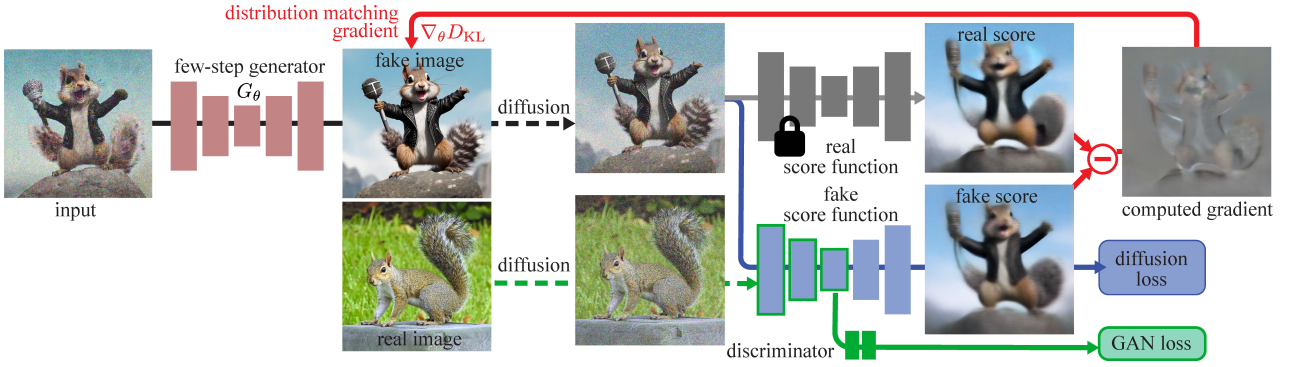


Figure 11: Overview of distribution matching distillation. Figure is adapted from [Yin et al., 2024a].

Variational Score Distillation Loss. Similar as in [Wang et al., 2024c], the variational score distillation (VSD) loss is designed to minimize the Kullback-Leibler (KL) of real (teacher) sample distribution p_{real} and fake (student) sample distribution p_{fake} , specifically:

$$\begin{aligned} \mathcal{L}_{\text{VSD}} &:= D_{\text{KL}}(p_{\text{fake}}||p_{\text{real}}) = \mathbb{E}_{x \sim p_{\text{fake}}} \left[\log \frac{p_{\text{fake}}(x)}{p_{\text{real}}(x)} \right] \\ &= \mathbb{E}_{\varepsilon \sim \mathcal{N}(0, \mathbf{I}), x = G_{\theta}(\varepsilon)} \left[\log \frac{p_{\text{fake}}(x)}{p_{\text{real}}(x)} \right] \end{aligned}$$

and the derivative of the objective is,

$$\nabla_{\theta} D_{\text{KL}} = \mathbb{E}_{\varepsilon \sim \mathcal{N}(0, \mathbf{I}), x = G_{\theta}(\varepsilon)} \left[-(s_{\text{real}}(x) - s_{\text{fake}}(x)) \nabla_{\theta} G_{\theta}(\varepsilon) \right] \quad (44)$$

with score functions $s_{\text{real}}(x) = \nabla_x \log p_{\text{real}}(x)$ and $s_{\text{fake}}(x) = \nabla_x \log p_{\text{fake}}(x)$ for two distributions. For practical estimation of the scores, the samples need to be diffused with noise to be x_t via forward diffusion. This gradient is essentially the same as the gradient of VSD objective. *The above scores are estimated with the diffusion model on their diffused distributions, as a sufficient condition for matching the corresponding scores on original real or fake distributions, according to the global optimum of VSD.*

Specifically, according to Eq. (17), given diffused distribution $q(x_t|x_0) \sim \mathcal{N}(x_t; \sqrt{\bar{\alpha}_t}x_0, (1 - \bar{\alpha}_t)\mathbf{I})$, the score $s_{\theta} = \nabla_{x_t} \log q(x_t)$ can be estimated with the diffusion model by:

$$s_{\theta}(x_t, t) = -\frac{x_t - \sqrt{\bar{\alpha}_t}x_{\theta}}{1 - \bar{\alpha}_t} \quad (45)$$

where $x_{\theta} = \frac{1}{\sqrt{\bar{\alpha}_t}}x_t - \frac{\sqrt{1-\bar{\alpha}_t}}{\sqrt{\bar{\alpha}_t}}\varepsilon_{\theta}$ is the reparameterization from ε -prediction to x_0 -prediction, using Eq. (6). There is also a shortcut to directly using $s_{\theta}(x_t, t) = -\frac{\varepsilon_{\theta}(x_t, t)}{\sqrt{1-\bar{\alpha}_t}}$ as Eq. (18), which yields the same results.

The practical operations for deriving the gradient update with VSD loss are:

1. Given data sample x_0 generated with G_{θ} , add noise ε to $x_{\tau}(\varepsilon)$ through forward diffusion as Eq. (27).

2. The student generator predicts denoised sample $x^f = G_\theta(x_\tau(\varepsilon))$, then forward diffuses it to $x_t^f(\varepsilon')$ with noise ε' with the same forward diffusion equation. Two different timestep sequences are applied. $\tau \in \{249, 499, 749, 999\}$ follows 4-step student sampling timesteps, while $t \in \{1, 2, \dots, 999\}$ follows teacher sampling timesteps.
3. Now calculate the real and fake score for $x_t^f(\varepsilon')$ using aforementioned score equation Eq. (45).

The real score $s^r(x_t^f)$ is computed using a frozen teacher model, while the fake score $s_\phi^f(x_t^f)$ is obtained from a copy of the teacher model with adaptive learning. The fake score model is updated through the diffusion loss during the distillation process to align with the distribution of the student-generated samples.

4. Take stochastic gradient descent to update the generator. Following Eq. (44), the gradient of distillation matching distillation loss has format:

$$\begin{aligned} \nabla_\theta \mathcal{L}_{\text{VSD}}(\theta) &= \mathbb{E}_{t, x_0, \varepsilon} [w(t) (s_\phi^f(x_t^f, t) - s^r(x_t^f, t))] \nabla_\theta G_\theta(x_\tau(\varepsilon)) \\ &= \nabla_\theta \mathbb{E}_{t, x_0, \varepsilon} \left[\frac{w(t)}{2} \|x^f - [x^f - (s_\phi^f(x_t^f, t) - s^r(x_t^f, t))].\text{detach()}\|^2 \right] \\ &= \nabla_\theta \mathbb{E}_{t, x_0, \varepsilon} \left[\frac{w(t)}{2} \frac{\sqrt{\bar{\alpha}_t}}{1 - \bar{\alpha}_t} \|x^f - [x^f - (x_\phi^f(x_t^f, t) - x^r(x_t^f, t))].\text{detach()}\|^2 \right] \end{aligned}$$

where $x_f = G_\theta(x_\tau(\varepsilon))$ and $w(t)$ is a time-dependent coefficient. The last equation is derived by score function Eq. (45), with $x_\phi^f(x_t^f, t)$ using the fake score model and $x^r(x_t^f, t)$ using the teacher model. The symbol “.detach()” indicates stopping the gradient in practice. In practice the weight coefficient is chosen as $w(t) = \frac{2(1-\bar{\alpha}_t)}{\sqrt{\bar{\alpha}_t}} \frac{c}{\|x_f - x^r(x_t^f, t)\|_1}$ with c as a constant of spatial and channel dimensions for better performances.

Diffusion Loss. Same as Eq. (42), the diffusion loss for fake score network s_ϕ^f follows standard diffusion model training for ϵ -prediction, x -prediction or v -prediction. Here we take ϵ -prediction as an example. The diffusion loss has form:

$$\mathcal{L}_{\text{diffusion}}(\phi) = \mathbb{E}_{x_0, t, \varepsilon} \|\varepsilon - \epsilon_\phi^f(F(x^f, t, \varepsilon))\|^2$$

$x_t^f(\varepsilon') = F(x^f, t, \varepsilon')$ with F as forward diffusion process. From Eq. (18), we know ϵ_ϕ^f and score s_ϕ^f can be mutually transformed by multiplying a simple coefficient.

Adversarial Loss. An additional GAN-type adversarial loss is introduced, leveraging a learned discriminator D_ψ . The adversarial loss has form:

$$\min_\theta \max_\psi \mathcal{L}_{\text{adv}}(\theta, \psi) = \mathbb{E}_{x'_0, t' \in [T], \varepsilon} [\log D_\psi(F(x'_0, t', \varepsilon))] + \mathbb{E}_{x_0, t \in [T], \varepsilon'} [-\log D_\psi(x_t^f(\varepsilon'))]$$

The forward diffusion function $F(x'_0, t', \varepsilon)$ generates a noisy sample from a clean sample x'_0 in the dataset, where $\varepsilon \sim \mathcal{N}(0, \mathbf{I})$ represents forward diffusion noise. The student-generated sample with noise is expressed as $x_t^f(\varepsilon') = F(x^f, t, \varepsilon') = F(G_\theta(x_\tau(\varepsilon)), t, \varepsilon')$. Note that the notations x'_0 and x_0 , t' and t , as well as ε and ε' , indicate that each pair can represent distinct values. The discriminator D_ψ shares the first half of the fake score network s_ϕ as its backbone. Alternatively,

it could share the backbone with the real score network (frozen), but this approach would result in only the discriminator head being updated, which may be insufficient for learning an accurate discriminator. Here, $t, t' \in \{1, 2, \dots, 999\}$.

Inference. Following the inference method of the consistency model, the process iteratively alternates between denoising and adding noise through forward diffusion, following a reverse sequence of timesteps $\{999, 749, 499, 249\}$ for 4-step sampling:

$$\begin{aligned}\hat{x}_0 &= G_\theta(x_{t_n}, t_n) && \text{(denoising)} \\ x_{t_{n-1}} &= \sqrt{\bar{\alpha}_{t_{n-1}}}\hat{x}_0 + \sqrt{1 - \bar{\alpha}_{t_{n-1}}}\varepsilon && \text{(forward diffusion)}\end{aligned}$$

3.2.5 Adversarial Diffusion Distillation

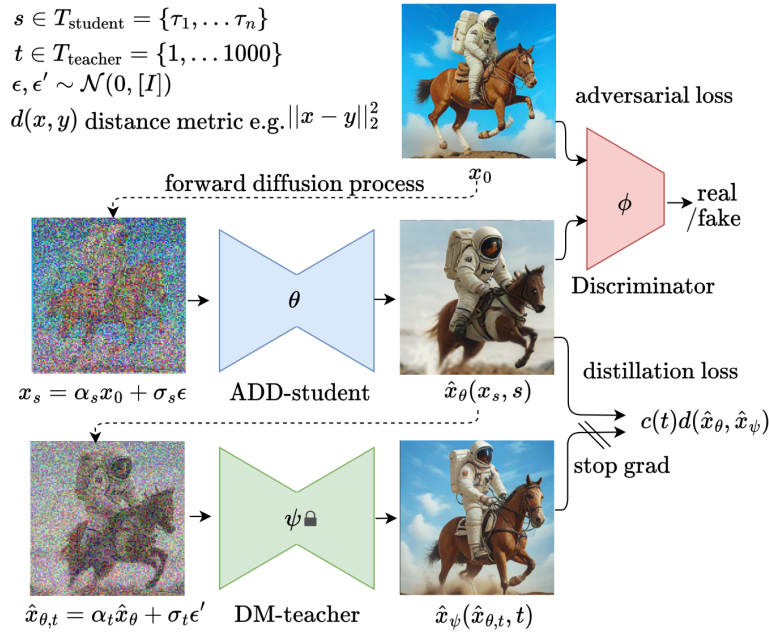


Figure 12: Overview of adversarial diffusion distillation. Figure is adapted from [Sauer et al., 2023].

As displayed in Fig. 12, adversarial diffusion distillation (ADD) [Sauer et al., 2023] combines adversarial loss and distillation loss:

$$\mathcal{L}_{\text{ADD}} = \mathcal{L}_{\text{adv}} + \lambda \mathcal{L}_{\text{distill}}$$

The adversarial loss follows standard GAN method, with a discriminator D_ϕ to distinguish between the student generated samples and real samples x_0 :

$$\min_{\theta} \max_{\phi} L_{\text{adv}}(\theta, \phi) = \mathbb{E}_{\varepsilon, s \in \{\tau_i\}_{i=1}^n, x_0} [\log D_\phi(\hat{x}_\theta(x_s, s)) + \log(1 - D_\phi(x_0))]$$

The distillation loss is to matching student and teacher prediction across timesteps:

$$\mathcal{L}_{\text{distill}} = \mathbb{E}_{t \in [T], s \in \{\tau_i\}_{i=1}^n} [c(t)d(\hat{x}_\theta(x_s, s), \hat{x}_\psi(x_t, t))]$$

where the student follows a sub-sequence of the teacher timesteps $\{\tau_i\}_{i=1}^n \subseteq [T]$, and $d(\cdot, \cdot)$ is a distance metric like MSE. $\hat{x}_\theta(x_s, s)$ and $\hat{x}_\psi(x_t, t)$ are predictions from student network ϵ_θ and teacher network ϵ_ψ respectively, following Eq. (7).

3.2.6 Consistency-based Distillation

The consistency model introduced in Sec. 2.3 can be applied for distillation from pre-trained diffusion model to reduce sampling steps.

Consistency Distillation. Consistency model [Song et al., 2023] enforces the consistency loss as the distillation method from a pre-trained teacher model $\epsilon_{\theta'}$, with a discrete sub-sampled time schedule $t_1 = \epsilon < t_2 < \dots < t_N = T$:

$$\begin{aligned} \mathcal{L}_{\text{CD}}(\theta) &= \mathbb{E}[\lambda(t_n)d(f_\theta(x_{t_{n+1}}, c, t_{n+1}), f_{\theta'}(\hat{x}_{t_n}, c, t_n))] \\ \hat{x}_{t_n} &= \text{Denoise}(x_{t_{n+1}}, c, t_{n+1}, t_n; \theta') \end{aligned} \quad (46)$$

where $\lambda(t_n)$ is a time dependent coefficient usually set as constant in practice, and $d(\cdot, \cdot)$ is a distance metric like MSE or Huber loss. One example of the one-step denoising function $\text{Denoise}(\cdot)$ is Eq. (21) for DDIM sampling with a pre-trained noise prediction diffusion model.

Latent Consistency Model (LCM) [Luo et al., 2023] introduces a way to reparameterize the f -prediction in consistency model with ϵ -prediction. Specifically, with a pre-trained teacher diffusion model $\epsilon_{\theta'}$, the student consistency model f_θ can be parameterized according to Eq. (24):

$$\begin{aligned} f_\theta(x_t, c, t) &= c_{\text{skip}}x_t + c_{\text{out}}x_\theta(x_t, c, t) \\ x_\theta &= \frac{x_t - \sqrt{1 - \bar{\alpha}_t}\epsilon_{\theta'}(x_t, c, t)}{\sqrt{\bar{\alpha}_t}} \end{aligned}$$

This allows student network ϵ_θ to be initiated with the teacher model $\epsilon_{\theta'}$ for leveraging the network compressed information during pre-training. If the student predicts other variables instead of the noise, the above reparameterization will take another form (see transformation between parameterization in Sec. 2.6). c is the condition variable in teacher network for conditional generation. To further enhance the conditioning capability, the classifier-free guidance (CFG) is applied:

$$\epsilon_\theta(x_t, c, t) = (1 + w)\epsilon_\theta(x_t, c, t) - w\epsilon_\theta(x_t, \emptyset, t)$$

The distilled student network also supports conditional generation with variable c but without CFG at inference.

This technique is applied in LCM [Luo et al., 2023], Animate LCM [Wang et al., 2024a], etc. Due to distilling from the teacher diffusion model, LCM methods drop the original noise schedule of CM but follow the noise schedule of teacher DM. Also, the student CM can take any subsequence $\{t_n\}_{n=1}^N$ of original timesteps $[T]$ during distillation and inference, which is natively supported by CM to achieve acceleration with reduced sampling steps. The inference pseudo-code is shown in Alg. 9.

Algorithm 9 LCM Inference

-
- 1: $x_{t_N} \sim \mathcal{N}(0, \mathbf{I}), \{t_n\}_{n=1}^N \subseteq [T]$
 - 2: **for** $n \in [N]$ **do**
 - 3: predict noise $\epsilon_\theta(x_{t_n}, c, t_n)$
 - 4: $\hat{x}_0 \leftarrow f_\theta(x_{t_n}, c, t_n)$ by consistency prediction Eq. (24)
 - 5: $x_{t_{n-1}} \leftarrow \sqrt{\bar{\alpha}_{t_{n-1}}}\hat{x}_0 + \sqrt{1 - \bar{\alpha}_{t_{n-1}}}\varepsilon, \varepsilon \sim \mathcal{N}(0, \mathbf{I})$
 - 6: **end for**
-

Generalized CD with multi-step denoising. The one-step CD loss can be generalized to m -step CD loss in practice, which changes Eq. (46) to be:

$$\begin{aligned} \mathcal{L}_{\text{CD}}(\theta) &= \mathbb{E}_{x_0 \sim q(x_0), t_n} [\lambda(t_n) d(f_\theta(x_{t_{n+m}}, c, t_{n+m}), f_{\theta^-}(\hat{x}_{t_n}, c, t_n))] \\ \hat{x}_{t_n} &= \text{Denoise}^m(x_{t_{n+m}}, c, t_{n+m}, t_n; \theta') \end{aligned} \quad (47)$$

with $\text{Denoise}^m(\cdot)$ indicating the m -step denoising function as defined by Eq. (22), which iteratively predicts the sequence $(\hat{x}_{t_{n+m-1}}, \dots, \hat{x}_{t_n} | x_{t_{n+m}})$.

Consistency Training for Distillation. We may also wonder if consistency training (CT), as another method for training consistency models, can help with the distillation process. The CT loss has the form:

$$\mathcal{L}_{\text{CT}}(\theta) = \mathbb{E}[\lambda(t_n) d(f_\theta(x_{t_{n+1}}, t_{n+1}), f_{\theta^-}(x_{t_n}, t_n))]$$

with $x_{t_{n+1}} = \sqrt{\bar{\alpha}_{t_{n+1}}}x_0 + \sqrt{1 - \bar{\alpha}_{t_{n+1}}}\varepsilon, x_{t_n} = \sqrt{\bar{\alpha}_{t_n}}x_0 + \sqrt{1 - \bar{\alpha}_{t_n}}\varepsilon, \varepsilon \sim \mathcal{N}(0, \mathbf{I})$, as forward diffusion process.

If the timestep schedule follows LCM with a constant interval $|t_{n+1} - t_n| = C$, one problem of above CT method for distillation is that it is not theoretically guaranteed to achieve a converging loss. From Theorem 2.2 we know, if $|t_{n+1} - t_n| \leq C$, then

$$\begin{aligned} \mathcal{L}_{\text{CD}}^N &= \mathcal{L}_{\text{CT}}^N + o(C) \\ \mathcal{L}_{\text{CT}}^N &\geq O(C) \text{ if } \inf \mathcal{L}_{\text{CD}}^N > 0 \end{aligned}$$

which yields a constant error $O(C)$ for $\mathcal{L}_{\text{CT}}^N$. Additionally, $o(C)$ is not asymptotically converging to 0 as C is not small (the Taylor expansion may not hold). This makes both CT and CD loss at least a constant error in theory. For above CT to converge, it requires a timestep schedule with asymptotically decreasing interval $|t_{n+1} - t_n| \leq o(C)$ as training iteration increases. LCM applies CD which directly minimizes $\mathcal{L}_{\text{CD}}^N$, therefore a constant timestep interval does not affect its convergence.

People may ask, instead of matching $f_\theta(x_{t_{n+1}}, t_{n+1})$ and $f_{\theta^-}(x_{t_n}, t_n)$, which accumulates error as t_n becomes large, why not directly matching $f_\theta(x_{t_n}, t_n)$ with x_0 . It follows the loss:

$$\mathcal{L}(\theta) = \mathbb{E}[\lambda(t_n) d(f_\theta(x_{t_n}, t_n), x_0)], n \in [N]$$

This actually corresponds to the diffusion loss for x -prediction, which can be readily proven. However, directly minimizing $d(f_\theta(x_{t_n}, t_n), x_0)$ does not require teacher guidance, and thus does not constitute distillation from any teacher model. Without leveraging the guidance of

the teacher along the diffusion path, training to predict $f_\theta(x_{t_n}) \rightarrow x_0$ becomes a challenging task, as the noise ϵ_θ to predict can vary significantly across different x_{t_n} . The teacher’s denoising function provides intermediate targets for the student to learn along the diffusion path, thereby alleviating the difficulty of learning (as a hypothetical statement).

To enable distillation from a pretrained teacher model with parameters θ' , the target x_0 in the above loss can be replaced with the teacher’s predicted $\hat{x}_0 = \text{Denoise}^n(x_{t_n})$, which requires an n -step denoising process. While this approach introduces potentially high computational costs, it provides a regression loss on teacher-generated samples, analogous to the regression loss used in distribution matching distillation [Yin et al., 2024b].

Student-Teacher Parameterization. Student-teacher parameterization can be categorized into two types: **homogeneous** and **heterogeneous**.

For homogeneous student-teacher parameterization, the student and teacher networks follow the same variable prediction, *e.g.*, both utilizing ϵ -prediction as in the LCM case described in Sec. 3.2.6.

For heterogeneous student-teacher parameterization, the student and teacher networks adopt different variable predictions, *e.g.*, ϵ -prediction for the teacher and v -prediction for the student. This setup necessitates an additional transformation between parameterizations, as discussed in Sec. 2.6.

For both types of parameterization, the student model can be initialized from the teacher model at the start of the distillation process, provided the network architectures are identical. However, homogeneous parameterization is expected to preserve more coherent weight information theoretically.

3.3 Reward-based Fine-tuning

Similar as reinforcement learning from human feedback (RLHF) in large language models, reward models can be used for fine-tuning pre-trained diffusion models. Based on whether the reward model’s gradient is utilized for optimization, reward fine-tuning methods can be categorized into two types: (1). direct reward gradient and (2). gradient-free reward optimization.

3.3.1 Direct Reward Gradient

We first introduce three methods requiring a differentiable reward model for gradient-based optimization, *i.e.*, $\nabla_x R(x)$, which includes ReFL, DRaFT and Q-score matching.

Reward Feedback Learning (ReFL) [Xu et al., 2024]. ReFL applies reward gradient for diffusion model optimization. It backpropagates the reward gradient through one-step predicted $x_\theta = \frac{1}{\sqrt{\alpha_t}}x_t - \frac{\sqrt{1-\alpha_t}}{\sqrt{\alpha_t}}\epsilon_\theta$ as Eq. (7), similar as diffusion posterior sampling [Chung et al., 2022]. The reward-based diffusion fine-tuning objective is:

$$\begin{aligned}\nabla_\theta \mathcal{L}_{\text{ReFL}} &= -\mathbb{E}_{\epsilon \sim \mathcal{N}(0, \mathbf{I})} [\nabla_\theta R_\phi(x_\theta)] \\ &= -\mathbb{E}_{\epsilon \sim \mathcal{N}(0, \mathbf{I})} [\nabla_{x_\theta} R_\phi(x_\theta) \nabla_\theta x_\theta]\end{aligned}$$

with R_ϕ as a differentiable reward model and ϵ_θ as the noise-prediction diffusion model.

Direct Reward Fine-Tuning (DRaFT) [Clark et al., 2023]. DRaFT requires the reward gradient to optimize the diffusion model, which optimize the following:

$$\begin{aligned}\nabla_{\theta}\mathcal{L}_{\text{DRaFT}} &= -\mathbb{E}_{\varepsilon\sim\mathcal{N}(0,\mathbf{I})}[\nabla_{\theta}R_{\phi}(G_{\theta}(\varepsilon))] \\ &= -\mathbb{E}_{\varepsilon\sim\mathcal{N}(0,\mathbf{I})}[\nabla_x R_{\phi}(x)\nabla_{\theta}G_{\theta}(\varepsilon)]\end{aligned}$$

where $x = G_{\theta}(\varepsilon)$ requires iterative sampling through the denoising function from noise ε . In practice, DRaFT usually requires truncation on gradient backpropagation along the diffusion chain, and find that truncating DRaFT to a single backwards step substantially improves sample efficiency. DRaFT- K truncates the reward gradient backpropagation in diffusion process to latest K steps as a trade-off between efficiency and performance.

Q-score Matching [Psenka et al., 2023]. The Q-score matching (QSM) proposes to directly match the score prediction from the diffusion model with the sample gradient from the value function (either reward or a Q-value in RL setting),

$$\mathcal{L}_{\text{QSM}}(\theta) = \mathbb{E}_{\varepsilon\sim\mathcal{N}(0,\mathbf{I}),t,x_t} \|s_{\theta}(x_t, t) - \nabla_{x_t}R(x_t)\|^2$$

with $s_{\theta}(x_t, t) = -\frac{x_t - \sqrt{\bar{\alpha}_t}\hat{x}_{\theta}}{1 - \bar{\alpha}_t}$. During usage, it requires to estimate reward values for x_t across all timesteps, $\forall t \in [T]$. This task can be ill-posed for the reward model, as it is typically designed to operate within the clean sample space, free from noise, *i.e.*, at $t = 0$.

3.3.2 Gradient-free Reward Optimization

Different from previous methods requiring reward gradients, we introduce other methods as “zero-th order” optimization without directly leveraging the reward gradients.

Denoising Diffusion Policy Optimization (DDPO) [Black et al., 2023]. Also inspired from REINFORCE algorithm, DDPO follows:

$$\begin{aligned}\nabla_{\theta}\mathcal{L}_{\text{DDPO}} &= -\mathbb{E}_{x_0\sim p_{\theta}(x_0)}[\nabla_{\theta}\log p_{\theta}(x_0)R(x_0)] \\ &= -\mathbb{E}_{\tau\sim p_{\theta}}\left[\sum_{t=1}^T\nabla_{\theta}\log p_{\theta}(x_{t-1}|x_t)R(x_0)\right] \\ &\quad (\text{with } p_{\theta}(x_0) = \int_{x_1}\cdots\int_{x_T}\prod_{t=1}^T p_{\theta}(x_{t-1}|x_t)dx_1dx_2\dots dx_T)\end{aligned}\tag{48}$$

where $\tau = \{x_T, x_{T-1}, \dots, x_0\}$, $x_T \sim \mathcal{N}(0, \mathbf{I})$. Notice that this requires to additionally marginalize out all intermediate variables $\tau_{T:1} = \{x_T, x_{T-1}, \dots, x_1\}$ generated along the diffusion chain, by the integral in expectation. In DDPM, the $p_{\theta}(x_{t-1}|x_t)$ is isotropic Gaussian following Eq. (8):

$$q(x_{t-1}|x_t, x_0) \propto \mathcal{N}\left(x_{t-1}; \frac{\sqrt{\bar{\alpha}_t}(1 - \bar{\alpha}_{t-1})x_t + \sqrt{\bar{\alpha}_{t-1}}(1 - \alpha_t)x_0}{1 - \bar{\alpha}_t}, \frac{(1 - \alpha_t)(1 - \bar{\alpha}_{t-1})}{1 - \bar{\alpha}_t}\mathbf{I}\right)$$

with

$$\mu_{\theta}(x_{t-1}|x_t, t) = \sqrt{\bar{\alpha}_{t-1}}\hat{x}_{\theta} + \sqrt{1 - \bar{\alpha}_{t-1} - \sigma_t^2}\epsilon_{\theta}(x_t, t)\tag{49}$$

$$\sigma_t = \sqrt{\frac{1 - \bar{\alpha}_{t-1}}{1 - \bar{\alpha}_t}} \sqrt{1 - \frac{\bar{\alpha}_t}{\bar{\alpha}_{t-1}}} \quad (50)$$

as previously proved in Eq. (12), and $\hat{x}_0 = \frac{x_t - \sqrt{1 - \bar{\alpha}_t} \epsilon_\theta}{\sqrt{\bar{\alpha}_t}}$. Then, the log-probability of Gaussian has explicit form:

$$\log p_\theta(x_{t-1}|x_t) = -\frac{(x_{t-1} - \mu_\theta)^2}{2\sigma_t^2} - \log \sigma_t - \log \sqrt{2\pi} \quad (51)$$

$$\nabla_\theta \log p_\theta(x_{t-1}|x_t) = \frac{\mu_\theta - x_{t-1}}{\sigma_t^2} \nabla_\theta \mu_\theta$$

DDPO requires per-step gradient estimation along the entire diffusion chain. But it does not require reward gradient or high-order sampling gradients along the diffusion chain.

The method as Eq. (48) here is DDPO_{SF}. This is the online version for gradient estimation, which requires to sample x_{t-1} as well as calculating the probabilities $p_\theta(x_{t-1}|x_t)$ along the sampling process at the same time, such that the model parameters θ remain the same for sampling and probability estimation. The update only takes one step to preserve the online estimation property. Original paper [Black et al., 2023] also proposes another version for offline policy gradient estimation with importance sampling to allow multi-step updates. The practical algorithm of DDPO_{SF} is shown in Alg. 10.

Algorithm 10 DDPO_{SF} practical procedure.

```

1: while train do
2:   //Sample from random noise along entire diffusion trajectory
3:    $x_T \leftarrow \epsilon \sim \mathcal{N}(0, \mathbf{I})$ 
4:   for  $t \in [T, \dots, 1]$  do
5:     Get posterior Gaussian  $(\mu_\theta, \sigma)$  with  $\epsilon_\theta(x_t.\text{detach}(), t)$  //Eq. (49) and (50)
6:     Sample  $x_{t-1} \sim \mathcal{N}(\mu_\theta, \sigma \mathbf{I})$ 
7:     Estimate  $\log p_\theta(x_{t-1}|x_t)$  //Eq. (51)
8:   end for
9:   Get reward  $R = R(\hat{x}_0).\text{detach}()$ 
10:  //REINFORCE policy gradient with truncation
11:   $\mathcal{L}_{\text{DDPO}_{\text{SF}}} = -\sum_n^N \log p_\theta(x_{t_{n-1}}.\text{detach}()|x_{t_n}) \cdot R$  //Eq. (48)
12:   $\theta \leftarrow \text{GradientDescent}(\theta, \mathcal{L}_{\text{DDPO}_{\text{SF}}})$ 
13: end while

```

Diffusion Reward-weighted Regression (DRWR) [Ren et al., 2024]. DRWR is a modified version of reward-weighted regression [Peters and Schaal, 2007] algorithm for reward-based optimization, using a weighted supervised learning objective.

$$\mathcal{L}_{\text{DRWR}}(\theta) = \mathbb{E}_{x, \epsilon, t} [\min(e^\beta R(x), w_{\max}) \|\epsilon - \epsilon_\theta(x, t)\|^2]$$

β and w_{\max} are scaling and clipping coefficients.

To reduce reward estimation variances and improve training stability, the reward value $R(x)$ can be replaced with the advantage estimation (in reinforcement learning terminology) through baseline subtraction: $A(x) = R(x) - R(\bar{x})$, following advantage-weighted regression [Peng et al., 2019]. Advanced reinforcement learning techniques like TD-bootstrapped advantage estimation can be further applied as in diffusion advantage-weighted regression (DAWR) method.

Acknowledgments

We thank Kexin Jin and Yuheng Zheng for their invaluable assistance in proofreading this draft and providing helpful feedback.

References

- [Albergo and Vanden-Eijnden, 2022] Albergo, M. S. and Vanden-Eijnden, E. (2022). Building normalizing flows with stochastic interpolants. *arXiv preprint arXiv:2209.15571*.
- [Anderson, 1982] Anderson, B. D. (1982). Reverse-time diffusion equation models. *Stochastic Processes and their Applications*, 12(3):313–326.
- [Black et al., 2023] Black, K., Janner, M., Du, Y., Kostrikov, I., and Levine, S. (2023). Training diffusion models with reinforcement learning. *arXiv preprint arXiv:2305.13301*.
- [Brooks et al., 2024] Brooks, T., Peebles, B., Holmes, C., DePue, W., Guo, Y., Jing, L., Schnurr, D., Taylor, J., Luhman, T., Luhman, E., et al. (2024). Video generation models as world simulators. 2024. URL <https://openai.com/research/video-generation-models-as-world-simulators>, 3.
- [Chung et al., 2022] Chung, H., Kim, J., Mccann, M. T., Klasky, M. L., and Ye, J. C. (2022). Diffusion posterior sampling for general noisy inverse problems. *arXiv preprint arXiv:2209.14687*.
- [Clark et al., 2023] Clark, K., Vicol, P., Swersky, K., and Fleet, D. J. (2023). Directly fine-tuning diffusion models on differentiable rewards. *arXiv preprint arXiv:2309.17400*.
- [Ho et al., 2020] Ho, J., Jain, A., and Abbeel, P. (2020). Denoising diffusion probabilistic models. *Advances in neural information processing systems*, 33:6840–6851.
- [Ho and Salimans, 2022] Ho, J. and Salimans, T. (2022). Classifier-free diffusion guidance. *arXiv preprint arXiv:2207.12598*.
- [Hyvärinen and Dayan, 2005] Hyvärinen, A. and Dayan, P. (2005). Estimation of non-normalized statistical models by score matching. *Journal of Machine Learning Research*, 6(4).
- [Karras et al., 2022] Karras, T., Aittala, M., Aila, T., and Laine, S. (2022). Elucidating the design space of diffusion-based generative models. *Advances in neural information processing systems*, 35:26565–26577.
- [Kingma, 2013] Kingma, D. P. (2013). Auto-encoding variational bayes. *arXiv preprint arXiv:1312.6114*.
- [Lipman et al., 2022] Lipman, Y., Chen, R. T., Ben-Hamu, H., Nickel, M., and Le, M. (2022). Flow matching for generative modeling. *arXiv preprint arXiv:2210.02747*.

- [Liu et al., 2023a] Liu, H., Chen, Z., Yuan, Y., Mei, X., Liu, X., Mandic, D., Wang, W., and Plumbley, M. D. (2023a). Audioldm: Text-to-audio generation with latent diffusion models. *arXiv preprint arXiv:2301.12503*.
- [Liu et al., 2022] Liu, X., Gong, C., and Liu, Q. (2022). Flow straight and fast: Learning to generate and transfer data with rectified flow. *arXiv preprint arXiv:2209.03003*.
- [Liu et al., 2023b] Liu, X., Zhang, X., Ma, J., Peng, J., et al. (2023b). InstafLOW: One step is enough for high-quality diffusion-based text-to-image generation. In *The Twelfth International Conference on Learning Representations*.
- [Lu and Song, 2024] Lu, C. and Song, Y. (2024). Simplifying, stabilizing and scaling continuous-time consistency models. *arXiv preprint arXiv:2410.11081*.
- [Luo et al., 2023] Luo, S., Tan, Y., Huang, L., Li, J., and Zhao, H. (2023). Latent consistency models: Synthesizing high-resolution images with few-step inference. *arXiv preprint arXiv:2310.04378*.
- [Meng et al., 2023] Meng, C., Rombach, R., Gao, R., Kingma, D., Ermon, S., Ho, J., and Salimans, T. (2023). On distillation of guided diffusion models. In *Proceedings of the IEEE/CVF Conference on Computer Vision and Pattern Recognition*, pages 14297–14306.
- [Peng et al., 2019] Peng, X. B., Kumar, A., Zhang, G., and Levine, S. (2019). Advantage-weighted regression: Simple and scalable off-policy reinforcement learning. *arXiv preprint arXiv:1910.00177*.
- [Peters and Schaal, 2007] Peters, J. and Schaal, S. (2007). Reinforcement learning by reward-weighted regression for operational space control. In *Proceedings of the 24th international conference on Machine learning*, pages 745–750.
- [Polyak et al., 2024] Polyak, A., Zohar, A., Brown, A., Tjandra, A., Sinha, A., Lee, A., Vyas, A., Shi, B., Ma, C.-Y., Chuang, C.-Y., et al. (2024). Movie gen: A cast of media foundation models. *arXiv preprint arXiv:2410.13720*.
- [Poole et al., 2022] Poole, B., Jain, A., Barron, J. T., and Mildenhall, B. (2022). Dreamfusion: Text-to-3d using 2d diffusion. *arXiv preprint arXiv:2209.14988*.
- [Psenka et al., 2023] Psenka, M., Escontrela, A., Abbeel, P., and Ma, Y. (2023). Learning a diffusion model policy from rewards via q-score matching. *arXiv preprint arXiv:2312.11752*.
- [Ramesh et al., 2022] Ramesh, A., Dhariwal, P., Nichol, A., Chu, C., and Chen, M. (2022). Hierarchical text-conditional image generation with clip latents. *arXiv preprint arXiv:2204.06125*, 1(2):3.
- [Ren et al., 2024] Ren, A. Z., Lidard, J., Ankile, L. L., Simeonov, A., Agrawal, P., Majumdar, A., Burchfiel, B., Dai, H., and Simchowitz, M. (2024). Diffusion policy optimization. *arXiv preprint arXiv:2409.00588*.
- [Rombach et al., 2022] Rombach, R., Blattmann, A., Lorenz, D., Esser, P., and Ommer, B. (2022). High-resolution image synthesis with latent diffusion models. In *Proceedings of the IEEE/CVF conference on computer vision and pattern recognition*, pages 10684–10695.

- [Salimans and Ho, 2022] Salimans, T. and Ho, J. (2022). Progressive distillation for fast sampling of diffusion models. *arXiv preprint arXiv:2202.00512*.
- [Sauer et al., 2023] Sauer, A., Lorenz, D., Blattmann, A., and Rombach, R. (2023). Adversarial diffusion distillation. *arXiv preprint arXiv:2311.17042*.
- [Sohl-Dickstein et al., 2015] Sohl-Dickstein, J., Weiss, E., Maheswaranathan, N., and Ganguli, S. (2015). Deep unsupervised learning using nonequilibrium thermodynamics. In *International conference on machine learning*, pages 2256–2265. PMLR.
- [Song et al., 2020a] Song, J., Meng, C., and Ermon, S. (2020a). Denoising diffusion implicit models. *arXiv preprint arXiv:2010.02502*.
- [Song and Dhariwal, 2023] Song, Y. and Dhariwal, P. (2023). Improved techniques for training consistency models. *arXiv preprint arXiv:2310.14189*.
- [Song et al., 2023] Song, Y., Dhariwal, P., Chen, M., and Sutskever, I. (2023). Consistency models. *arXiv preprint arXiv:2303.01469*.
- [Song and Ermon, 2019] Song, Y. and Ermon, S. (2019). Generative modeling by estimating gradients of the data distribution. *Advances in neural information processing systems*, 32.
- [Song and Ermon, 2020] Song, Y. and Ermon, S. (2020). Improved techniques for training score-based generative models. *Advances in neural information processing systems*, 33:12438–12448.
- [Song et al., 2020b] Song, Y., Sohl-Dickstein, J., Kingma, D. P., Kumar, A., Ermon, S., and Poole, B. (2020b). Score-based generative modeling through stochastic differential equations. *arXiv preprint arXiv:2011.13456*.
- [Song et al., 2021] Song, Y., Sohl-Dickstein, J., Kingma, D. P., Kumar, A., Ermon, S., and Poole, B. (2021). Score-based generative modeling through stochastic differential equations. In *International Conference on Learning Representations*.
- [Vincent, 2011] Vincent, P. (2011). A connection between score matching and denoising autoencoders. *Neural computation*, 23(7):1661–1674.
- [Wang et al., 2024a] Wang, F.-Y., Huang, Z., Shi, X., Bian, W., Song, G., Liu, Y., and Li, H. (2024a). Animatelem: Accelerating the animation of personalized diffusion models and adapters with decoupled consistency learning. *arXiv preprint arXiv:2402.00769*.
- [Wang et al., 2024b] Wang, Y., Wang, X., Chen, Z., Wang, Z., Sun, F., and Zhu, J. (2024b). Vidu4d: Single generated video to high-fidelity 4d reconstruction with dynamic gaussian surfels. *arXiv preprint arXiv:2405.16822*.
- [Wang et al., 2024c] Wang, Z., Lu, C., Wang, Y., Bao, F., Li, C., Su, H., and Zhu, J. (2024c). Prolificdreamer: High-fidelity and diverse text-to-3d generation with variational score distillation. *Advances in Neural Information Processing Systems*, 36.
- [Weng, 2021] Weng, L. (2021). What are diffusion models? *lilianweng.github.io*.

- [Xu et al., 2024] Xu, J., Liu, X., Wu, Y., Tong, Y., Li, Q., Ding, M., Tang, J., and Dong, Y. (2024). Imagereward: Learning and evaluating human preferences for text-to-image generation. *Advances in Neural Information Processing Systems*, 36.
- [Yin et al., 2024a] Yin, T., Gharbi, M., Park, T., Zhang, R., Shechtman, E., Durand, F., and Freeman, W. T. (2024a). Improved distribution matching distillation for fast image synthesis. *arXiv preprint arXiv:2405.14867*.
- [Yin et al., 2024b] Yin, T., Gharbi, M., Zhang, R., Shechtman, E., Durand, F., Freeman, W. T., and Park, T. (2024b). One-step diffusion with distribution matching distillation. In *Proceedings of the IEEE/CVF Conference on Computer Vision and Pattern Recognition*, pages 6613–6623.
- [Zhang et al., 2018] Zhang, R., Isola, P., Efros, A. A., Shechtman, E., and Wang, O. (2018). The unreasonable effectiveness of deep features as a perceptual metric. In *Proceedings of the IEEE conference on computer vision and pattern recognition*, pages 586–595.